Amplitude Higgs mode in superconductors with magnetic impurities

Yantao Li and Maxim Dzero
Department of Physics, Kent State University, Kent, Ohio 44242, USA

(Received 4 December 2023; accepted 6 February 2024; published 22 February 2024; corrected 28 October 2024)

We study the nonlinear response of conventional superconducting alloys with weak magnetic impurities to an external alternating electromagnetic field. In particular, we calculate a correction to the superconducting order parameter $|\delta\Delta_\Omega|\exp(i\Omega t)$ up to second order in the external vector potential and show that the frequency dependence of the order parameter amplitude has a characteristic resonant shape with a maximum at the frequency which is smaller than twice the magnitude of the pairing amplitude in equilibrium, $\Omega < 2\Delta$, and at the same time exceeds the single-particle threshold energy. Our results suggest that in the presence of magnetic impurities the dynamics of the pairing amplitude in the collisionless regime will remain robust with respect to dissipative processes. We also evaluate the third harmonic contribution to the current as a function of the probe frequency and for various concentrations of magnetic impurities.

DOI: 10.1103/PhysRevB.109.054520

I. INTRODUCTION

Recent advances in state-of-the-art optical instruments and techniques have led to increased interest in problems which focus on theoretical and experimental studies of various nonlinear responses in conventional and unconventional superconductors [1–6]. It is worth noting that while these developments must have been motivated, at least in part, by earlier theoretical discoveries such as stimulation of superconductivity by microwave radiation (Eliashberg effect) and collisionless dynamics of the pairing amplitude in conventional BCS superconductors [7–12], the main conceptual motivation to make significant advances in this area of research has come from the realization that a similarity exists between cosmology and condensed matter physics, specifically to superconductivity as well as other phases which exhibit well-defined long-range order [13–18]. Indeed, the fully gapped amplitude mode in superconductors is similar to the Higgs mode in quantum field theories [19–23]. Therefore, by exploiting this similarity it becomes, in principle, feasible to probe the physics associated with the amplitude mode in a tabletop experimental setup [24].

The excitation and propagation of the amplitude mode in superconductors are completely decoupled from the charge density fluctuations which are related to the phase fluctuations of the pairing field [23]. On timescales which are short in comparison with the characteristic timescales for single-particle relaxation processes, the dynamics of the pairing amplitude is described by kinetic equations in which the collision integrals $I_{\text{e-e}} \propto \hbar/\tau_{\text{e-e}}$ and $I_{\text{e-ph}} \propto \hbar/\tau_{\text{e-ph}}$, which account for the electron-electron and electron-phonon scattering effects, respectively, can be ignored [10,25–30]. In other words, the dynamics of the amplitude mode is considered in the collisionless regime. Therefore, the problem of pairing amplitude dynamics becomes conceptually analogous to that of the collisionless relaxation of an electric field in electronic plasma [31,32]. Curiously, while the electric field in electronic plasma attenuates exponentially fast after an initial perturbation (Landau damping), in conventional superconductors the amplitude mode asymptotes to a constant according to a power law [10,33,34]:

$$|\Delta(t)| = \Delta_\infty\left(1 + a\frac{\cos(2\Delta_\infty t + \pi/4)}{\sqrt{2\Delta_\infty t}}\right), \tag{1}$$

where a is some known parameter. The physical origin of this behavior has been understood using the exact solution to the problem of the BCS dynamics in fermionic condensates [27–29,35,36]. Following the initial perturbation, collective modes with frequencies $2\Omega_j = 2(\epsilon_j^2 + \Delta^2)^{1/2}$ are excited (ϵ_j are the roots of a certain nonlinear equation [34]), and in complete analogy with the problem considered by Landau [31,32,37], the dynamics of the pairing amplitude will be determined by a sum over excitation energies. In concert with the square-root anomaly in the density of states, this summation ultimately produces a power-law decay of the pairing amplitude, Eq. (1), provided, of course, that the deviations from equilibrium are not too large [34].

It is important for our subsequent discussion to keep in mind that in the linear approximation, i.e., when the initial perturbation is weak (e.g., quenches of the pairing strength g are of small magnitude, $|\delta g| \ll g$), Δ_∞ is equal to the value of the pairing amplitude in equilibrium Δ [38]. Therefore, in the context of the pump-probe experiments one would expect the resonant amplitude Higgs mode to be excited when the external frequency of the monochromatic field is tuned to $2\Omega_{\text{res}} = 2\Delta$ [37,39–45]. Alternatively, when the superconductor is in a state which carries a supercurrent, the amplitude Higgs mode will be excited at resonant frequency $\Omega_{\text{res}} = 2\Delta$ [23].

There is a question of whether the effects of potential disorder will affect the results we just discussed for clean superconductors in any way. For zero-dimensional systems it is obvious that potential disorder will produce the renormalization of the single-particle energy levels and therefore will have no effect on the dynamics of the amplitude mode. In three-dimensional systems the situation is more subtle. For a case of weak disorder the Anderson theorem [46] guarantees that potential disorder should not have a significant effect on the dynamics, and this conclusion should hold in both the ballistic and diffusive regimes [47–51]. Larkin and Ovchinnikov [52] showed that when disorder is strong enough to render the pairing interaction spatially inhomogeneous, in this case the inhomogeneities lead to pair breaking, and at the mean-field level, their theory becomes analogous to the Abrikosov-Gor'kov theory of superconductors contaminated with paramagnetic impurities [53]. It is therefore expected that in this case amplitude dynamics may exhibit qualitatively different behavior from Eq. (1), and the results of the recent experiments on superconducting films near the superconductor-insulator transition [54] seem to be in agreement with these observations, although systematic theoretical analysis of these systems is inhibited by the fact that the ground state in strongly disordered superconducting films still remains very poorly understood [55,56].

Although the effects of potential disorder on an amplitude mode had already been studied, the question of what happens to the dynamics of the amplitude mode in superconducting alloys with magnetic impurities was not addressed until very recently [57]. This is quite surprising given how conceptually rich the problem of the interplay between conventional superconductivity and paramagnetic disorder really is (see, e.g., [58–65] and references therein). Experimental progress in this direction is, perhaps, inhibited by the fact that it may be challenging to introduce magnetic impurities in a controlled way such that their interplay with the dynamics of an amplitude mode can be probed in the collisionless regime.

One of the main results of [57] consists of the following observation: When the relaxation time τ_s due to the scattering of conduction electrons on paramagnetic impurities is long enough that the conditions $\tau_s \ll \tau_{\rm ee}$ and $\zeta = 1/\tau_s\Delta \ll 1$ are met, after a quench of an arbitrarily small magnitude (linear approximation), the dynamics of the amplitude Higgs mode on the timescale $\tau_s \ll t \ll \tau_{\rm ee}$ remains undamped,

$$|\Delta(t)| = \Delta\{1 + \zeta\cos(\omega_s t + \pi/4)\}, \tag{2}$$

even though on shorter timescales $\tau_\Delta \ll t \ll \tau_s$ it approximately follows the Volkov-Kogan asymptotic formula (1). The frequency of the Higgs mode oscillations is given by $\omega_s \approx 2\Delta\sqrt{1-\zeta^2} < 2\Delta$. Clearly, Eq. (2) is very different from the Volkov-Kogan result, Eq. (1), and it implies that scattering on paramagnetic impurities pushes the frequency of the Higgs mode below the minimum of the band of excitation energies Ω_j, rendering it nondissipative. In passing we note that in clean superconductors the realization of a state with an oscillating amplitude requires fairly large deviations from equilibrium [25,30,36,66,67], which makes the result (2), given that it appears already in the linear approximation, even more striking. We would like to emphasize that the results of Ref. [57] are valid in only the perturbative regime, $\zeta \ll 1$. Naturally, there are still questions which remain unanswered, such as the one about the fate of this nondissipative amplitude mode when $\zeta \sim 1$, especially in the regime of gapless superconductivity [58]. Last, we note that similar findings were recently reported in the context of a problem in which a clean superconductor is coupled to a strongly driven cavity [68], where the external electromagnetic field in the cavity pushes the frequency of the Higgs mode below the gap edge and causes the order parameter dynamics to become periodic in time.

In Ref. [57] the out-of-equilibrium dynamics in the s-wave superconductor was induced by a sudden, albeit small, change in the pairing strength. In this paper we consider a realistic situation in which the out-of-equilibrium dynamics is induced by an external electromagnetic ac field and compute the frequency dependence of the amplitude Higgs mode. We show that the resonance frequency at which this mode is excited is, indeed, smaller than 2Δ. At the same time, by evaluating the single-particle density of states we demonstrate that it remains above the single-particle threshold $\Delta_{\rm th} = \Delta(1-\zeta^{2/3})^{3/2}$. These results are in general agreement with those of Ref. [57]. In addition we compute the third harmonic contribution to the current in the pump-probe setup as a function of the probe frequency assuming the pump frequency has been tuned to the vicinity of the resonance amplitude mode frequency. We find that the largest contribution to the third harmonic is governed by the amplitude mode. We also find that the third harmonic contribution to the current is suppressed with an increase in the magnetic scattering rate. We think that this particular result may shed some light on the physical origin of the energy scale corresponding to the resonant frequency of the amplitude mode. We emphasize that our present findings are generally applicable for arbitrary values of the dimensionless parameter ζ. However, the effects associated with the formation of the Yu-Shiba-Rusinov bound states are not included in our forthcoming discussion and will be considered separately.

II. BASIC EQUATIONS

In what follows we consider a disordered BCS superconductor in the diffusive limit $\Delta \ll 1/\tau$, where τ is the relaxation time due to scattering on potential impurities. It is clear that in the presence of the magnetic impurities this condition can always be fulfilled. At the same time we will assume that $\tau \ll \tau_s$.

The central quantity for our analysis is the Green's function defined on the Keldysh contour:

$$\check{G}(t,t') = \begin{pmatrix} \hat{G}^R(t,t') & \hat{G}^K(t,t') \\ 0 & \hat{G}^A(t,t') \end{pmatrix}. \tag{3}$$

Each component of the matrix function $\check{G}$ is a 4×4 matrix and Nambu and spin subspaces [60,69]. The Green's function (3) can be found by solving the Usadel equation for disordered superconductors, which corresponds to a spatially homogeneous configuration of the Q matrix at the saddle point of the nonlinear σ model [70,71]:

$$i\big(\check{\Xi}_3\partial_t\check{G} + \partial_{t'}\check{G}\check{\Xi}_3\big) + [\check{\Delta},\check{G}] + \frac{i}{6\tau_s}[(\hat{\rho}_3\otimes\hat{\sigma}_i)\check{G}(\hat{\rho}_3\otimes\hat{\sigma}_i) \,\overset{\circ}{,}\, \check{G}] = -iD[\check{\mathbf{Q}}\check{G}\check{\mathbf{Q}} \,\overset{\circ}{,}\, \check{G}]. \tag{4}$$

Here $D = v_F^2\tau/3$ is the diffusion coefficient, $\check{\mathbf{Q}}(t) = (\hat{\gamma}_0\otimes\hat{\Xi}_3)\mathbf{A}(t)$, $\mathbf{A}(t)$ is proportional to an external vector potential, $\check{\Xi}_3 = \hat{\gamma}_0\otimes\hat{\Xi}_3$ is diagonal in the Keldysh subspace, $\hat{\gamma}_0$ is the unit Pauli matrix in the Keldysh space, $\hat{\Xi}_3 = \hat{\rho}_3\otimes\hat{\sigma}_0$,

$(\check{A}\circ\check{B})(t,t')=\int dt_1\check{A}(t,t_1)\check{B}(t_1,t')$, and $\hat{\rho}_n$ and $\hat{\sigma}_m$ $(n,m=1,2,3)$ are the Pauli matrices acting in the Nambu and spin subspaces, respectively. Function $\check{G}$ must satisfy the normalization condition

$$\check{G}\circ\check{G}=\check{\mathbb{1}},\tag{5}$$

and the third term in this equation should be understood as $[\check{\Delta},\check{G}]=\check{\Delta}(\mathbf{r},t)\check{G}(\mathbf{r};t,t')-\check{G}(\mathbf{r};t,t')\check{\Delta}(\mathbf{r},t')$, where the matrix $\check{\Delta}(\mathbf{r},t)=\Delta(\mathbf{r},t)(\hat{\gamma}_0\otimes i\hat{\rho}_2\otimes\sigma_0)$ is diagonal in the Keldysh space. The pairing field must be computed self-consistently from

$$\Delta(t)=\frac{\pi\lambda}{2}\mathrm{Tr}\{[\hat{\gamma}_1\otimes(\hat{\rho}_1-i\hat{\rho}_2)\otimes\hat{\sigma}_0]\check{G}(t,t)\}.\tag{6}$$

Here λ is the dimensionless pairing strength, and $\hat{\gamma}_1$ is the first Pauli matrix acting in the Keldysh subspace. We would like to emphasize that Eq. (4) was found by performing exact averaging over potential and magnetic disorder configurations. The only approximation that we have made is similar to one made in Refs. [60,61] for the contribution from scattering on magnetic impurities. This approximation is justified in the limit $\tau\ll\tau_s$. In other words, the spatially homogeneous solution of (4) is applicable within the validity of the self-consistent Born approximation.

A. Ground state

The expressions for the components of $\check{G}(t,t')$ in the ground state are found by solving the Usadel equation (4) when the external field is set to zero:

$$i(\check{\Xi}_3\partial_t\check{\mathcal{G}}+\partial_{t'}\check{\mathcal{G}}\check{\Xi}_3)+[\check{\Delta},\check{\mathcal{G}}]\\+\frac{i}{6\tau_s}\sum_{a=1}^{3}[(\hat{\rho}_3\otimes\hat{\sigma}_a)\check{\mathcal{G}}(\hat{\rho}_3\otimes\hat{\sigma}_a)\circ,\check{\mathcal{G}}]=0.\tag{7}$$

Performing the Fourier transform for the first term, we find

$$i(\check{\Xi}_3\partial_t\check{\mathcal{G}}+\partial_{t'}\check{\mathcal{G}}\check{\Xi}_3)=\int\frac{\epsilon d\epsilon}{2\pi}(\check{\Xi}_3\check{\mathcal{G}}_\epsilon-\check{\mathcal{G}}_\epsilon\check{\Xi}_3)e^{-i\epsilon(t-t')}.\tag{8}$$

As is well known, at equilibrium the Keldysh sub-block $\hat{\mathcal{G}}^K$ can always be chosen to be

$$\hat{\mathcal{G}}_\epsilon^K=(\hat{\mathcal{G}}_\epsilon^R-\hat{\mathcal{G}}_\epsilon^A)\tanh\left(\frac{\epsilon}{2T}\right).\tag{9}$$

From the normalization condition (5) we find

$$\hat{\mathcal{G}}_\epsilon^R\hat{\mathcal{G}}_\epsilon^R=\hat{\mathbb{1}},\quad\hat{\mathcal{G}}_\epsilon^A\hat{\mathcal{G}}_\epsilon^A=\hat{\mathbb{1}},\quad\hat{\mathcal{G}}_\epsilon^R\hat{\mathcal{G}}_\epsilon^K+\hat{\mathcal{G}}_\epsilon^K\hat{\mathcal{G}}_\epsilon^A=0.\tag{10}$$

Below we will determine each of these Green's functions separately.

1. Retarded and advanced Green's functions

Let us discuss an equation for the retarded matrix function $\hat{\mathcal{G}}_\epsilon^R$ first. From the form of the Usadel equation, we look for the solution for this function in the form

$$\hat{\mathcal{G}}_\epsilon^R=g_\epsilon^R\hat{\Xi}_3+f_\epsilon^R\hat{\Xi}_2.\tag{11}$$

Here we introduced the matrix $\hat{\Xi}_2=i\hat{\rho}_2\otimes\hat{\sigma}_0$. Inserting this expression into Eq. (7) yields

$$\left(\epsilon+\frac{ig_\epsilon^R}{2\tau_s}\right)f_\epsilon^R-\left(\Delta-\frac{if_\epsilon^R}{2\tau_s}\right)g_\epsilon^R=0.\tag{12}$$

This equation is supplemented by the normalization condition $(g_\epsilon^R)^2-(f_\epsilon^R)^2=1$. We can use the following standard parametrization for the functions $g_\epsilon^R=\cosh\theta_\epsilon$ and $f_\epsilon^R=\sinh\theta_\epsilon$. Introducing auxiliary variables $\tilde{\epsilon}=\epsilon+(i/2\tau_s)\cosh\theta_\epsilon$ and $\tilde{\Delta}_\epsilon=\Delta-(i/2\tau_s)\sinh\theta_\epsilon$, we employ the normalization condition to write down the formal solution of (12):

$$\cosh\theta_\epsilon=\frac{u_\epsilon}{\sqrt{u_\epsilon^2-1}},\quad\sinh\theta_\epsilon=\frac{1}{\sqrt{u_\epsilon^2-1}},\quad u_\epsilon=\frac{\tilde{\epsilon}}{\tilde{\Delta}_\epsilon}.\tag{13}$$

Note that in the limit $\epsilon\gg\Delta$, it is implied that $u_\epsilon^{R(A)}=\pm\mathrm{sgn}\epsilon$.

Equations (13) are not a solution, just another parametrization of the Green's functions (11). The actual solution of the Usadel equation determines the dependence of g_ϵ^R and f_ϵ^R on energy ϵ; hence, u is a function of ϵ as well. The equation which allows one to compute the dependence of u_ϵ on ϵ reads

$$u_\epsilon\left(1-\frac{1}{\tau_s\Delta}\frac{1}{\sqrt{1-u_\epsilon^2}}\right)=\frac{\epsilon}{\Delta}.\tag{14}$$

Thus, in what follows, we assume that the solution of Eq. (14) is known and will work with the retarded and advanced Green's functions:

$$\hat{\mathcal{G}}_\epsilon^R=\left(\frac{u_\epsilon}{\sqrt{u_\epsilon^2-1}}\hat{\Xi}_3+\frac{1}{\sqrt{u_\epsilon^2-1}}\hat{\Xi}_2\right)\mathrm{sgn}(\epsilon),$$
$$\hat{\mathcal{G}}_\epsilon^A=-\hat{\Xi}_3(\hat{\mathcal{G}}_\epsilon^R)^\dagger\hat{\Xi}_3=-\frac{\overline{u}_\epsilon\mathrm{sgn}(\epsilon)}{\sqrt{\overline{u}_\epsilon^2-1}}\hat{\Xi}_3-\frac{\mathrm{sgn}(\epsilon)}{\sqrt{\overline{u}_\epsilon^2-1}}\hat{\Xi}_2.\tag{15}$$

Here $\overline{u}_\epsilon=u_\epsilon^*$ implies complex conjugation. Equation (14) can easily be solved, which allows one to compute the single-particle density of states (DOS) per spin,

$$\frac{\nu(\epsilon)}{\nu_0}=\mathrm{Re}\frac{u_\epsilon}{\sqrt{u_\epsilon^2-1}},\tag{16}$$

and the value of the order parameter at a given temperature:

$$\Delta=\lambda\int_{-\omega_D}^{\omega_D}d\epsilon\left(f_\epsilon^R-f_\epsilon^A\right)\tanh\left(\frac{\epsilon}{2T}\right).\tag{17}$$

Here (16) ν_0 is the electron DOS per spin projection at the Fermi level in the normal state, and ω_D is the Debye frequency. We present plots of $\nu(\epsilon)$ and Δ for various values of $\zeta=1/\tau_s\Delta$ in Fig. 1.

B. Application of an external electromagnetic field

Having computed the Green's function in the ground state, we now look for the correction to the Green's function due to an application of external field. We represent the external vector potential as a superposition of two monochromatic waves,

$$\mathbf{A}(t)=\mathbf{A}_{\Omega_1}e^{i\Omega_1t}+\mathbf{A}_{\Omega_2}e^{i\Omega_2t}+\mathrm{c.c.}\tag{18}$$

Our calculation will closely follow the path of Refs. [23,37]. Specifically, we consider a correction to the Green's function $\check{\mathcal{G}}_\epsilon$,

$$\check{G}(\epsilon,\epsilon')=2\pi\check{\mathcal{G}}_\epsilon\delta(\epsilon-\epsilon')+\check{g}_1(\epsilon,\epsilon'),\tag{19}$$

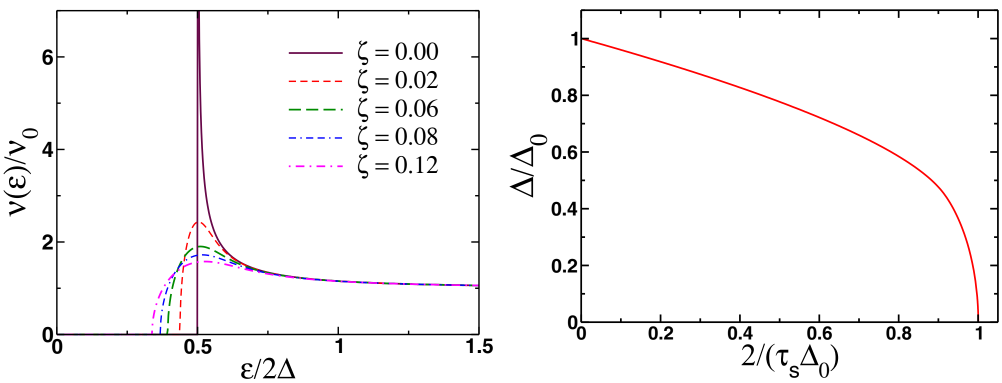

FIG. 1. Left: Single-particle density of states per spin as a function of energy (16) evaluated for various values of the dimensionless parameter $\zeta = 1/\tau_s\Delta$. Right: Order parameter Δ as a function of the disorder scattering rate $1/\tau_s$.

and a correction to the order parameter, $\check{\Delta}(t) = \check{\Delta} + \check{\Delta}_1(t)$. The value of the unperturbed order parameter $\check{\Delta}$ must be computed self-consistently using Eq. (6). Also, from the normalization condition it follows that the components of $\check{g}_1$ must satisfy

$$\check{\mathcal{G}}_\epsilon \check{g}_1(\epsilon, \epsilon') + \check{g}_1(\epsilon, \epsilon')\check{\mathcal{G}}_{\epsilon'} = 0. \tag{20}$$

In the ground state we assume that the order parameter is real. Under the action of the external field it may acquire an imaginary part. That is why the most general form of the three Keldysh blocks in the matrix Green's function $\check{g}_1$ must be of the form

$$\hat{g}_1(\epsilon, \epsilon') = g_1(\epsilon, \epsilon')\hat{\Xi}_3 + f_1(\epsilon, \epsilon')\hat{\Xi}_2. \tag{21}$$

Note that due to the matrix form of (21), the corresponding matrix form of $\hat{\Delta}_1$ is the same as that of $\hat{\Delta}$.

Now we go back to Eq. (4) and insert (19) into the left-hand side of that equation. We keep the terms linear in $\check{g}_1$, and after performing the Fourier transformation we obtain

$$\begin{aligned}
&(\epsilon\check{\Xi}_3 + \check{\Delta})\check{g}_1(\epsilon, \epsilon') - \check{g}_1(\epsilon, \epsilon')(\epsilon'\check{\Xi}_3 + \check{\Delta})\\
&\quad + \check{\Delta}_1(\epsilon' - \epsilon)\check{\mathcal{G}}_{\epsilon'} - \check{\mathcal{G}}_\epsilon\check{\Delta}_1(\epsilon' - \epsilon)\\
&\quad + \frac{i}{6\tau_s}\sum_a \check{\Theta}_a\check{\mathcal{G}}_\epsilon\check{\Theta}_a\check{g}_1(\epsilon, \epsilon') - \frac{i}{6\tau_s}\sum_a \check{g}_1(\epsilon, \epsilon')\check{\Theta}_a\check{\mathcal{G}}_{\epsilon'}\check{\Theta}_a\\
&= -2\pi i D\sum_{\mu\nu}(\check{\mathbf{Q}}_\nu\check{\mathcal{G}}_{\epsilon+\Omega_\nu}\check{\mathbf{Q}}_\mu\check{\mathcal{G}}_{\epsilon'} - \check{\mathcal{G}}_\epsilon\check{\mathbf{Q}}_\nu\check{\mathcal{G}}_{\epsilon'-\Omega_\mu}\check{\mathbf{Q}}_\mu)\\
&\quad \times \delta(\epsilon' - \epsilon - \Omega_{\nu+\mu}),
\end{aligned} \tag{22}$$

where $\check{\Theta}_a = (\hat{\gamma}_0 \otimes \hat{\rho}_3 \otimes \hat{\sigma}_a)$, $\Omega_{\nu,\mu} = \pm\Omega_{1,2}$, and $\Omega_{\nu+\mu} = \Omega_\nu + \Omega_\mu$.

Some rearrangements of the few terms in this equation are in order. Let us first look at the third and fourth terms on the left-hand side of this equation: They have the same structure as the one on the right-hand side. From the expression on the right-hand side, we note that the electromagnetic field will have an effect only when

$$\epsilon' - \epsilon = \Omega_{\nu+\mu}. \tag{23}$$

In other words, $\check{\Delta}_1(\epsilon' - \epsilon)$ is nonzero only when (23) holds. Then we use this observation to rewrite the third and fourth terms as

$$\begin{aligned}
&\check{\Delta}_1(\epsilon' - \epsilon)\check{\mathcal{G}}_{\epsilon'} - \check{\mathcal{G}}_\epsilon\check{\Delta}_1(\epsilon' - \epsilon)\\
&\quad = 2\pi\sum_{\nu\mu}[\check{\Delta}_1(\Omega_{\nu+\mu})\check{\mathcal{G}}_{\epsilon'} - \check{\mathcal{G}}_\epsilon\check{\Delta}_1(\Omega_{\nu+\mu})]\\
&\quad \times \delta(\epsilon' - \epsilon - \Omega_{\nu+\mu}).
\end{aligned} \tag{24}$$

The remaining terms on the left-hand side can be simplified. Indeed, when $\tau_s \to \infty$, it is easy to see that $(\epsilon\check{\Xi}_3 + \check{\Delta}) \propto [\check{\mathcal{G}}_\epsilon]_{\tau_s\to\infty}$. Taking these expressions into account, we can now rewrite (22) as follows:

$$\begin{aligned}
&\check{\Gamma}_\epsilon\check{g}_1(\epsilon, \epsilon') - \check{g}_1(\epsilon, \epsilon')\check{\Gamma}_{\epsilon'}\\
&\quad = 2\pi\sum_{\nu\mu}[\check{\mathcal{R}}_Q(\epsilon, \epsilon') + \check{\mathcal{R}}_\Delta(\epsilon, \epsilon')]\delta(\epsilon' - \epsilon - \Omega_{\nu+\mu}).
\end{aligned} \tag{25}$$

Here we introduce the following matrix functions:

$$\begin{aligned}
&\check{\mathcal{R}}_Q(\epsilon, \epsilon') = iD(\check{\mathcal{G}}_\epsilon\check{\mathbf{Q}}_\nu\check{\mathcal{G}}_{\epsilon'-\Omega_\mu}\check{\mathbf{Q}}_\mu - \check{\mathbf{Q}}_\nu\check{\mathcal{G}}_{\epsilon+\Omega_\nu}\check{\mathbf{Q}}_\mu\check{\mathcal{G}}_{\epsilon'}),\\
&\check{\mathcal{R}}_\Delta(\epsilon, \epsilon') = \check{\mathcal{G}}_\epsilon\check{\Delta}_1(\Omega_{\nu+\mu}) - \check{\Delta}_1(\Omega_{\nu+\mu})\check{\mathcal{G}}_{\epsilon'},\\
&\check{\Gamma}_\epsilon = \epsilon\check{\Xi}_3 + \check{\Delta} + \frac{i}{6\tau_s}\sum_{a=1}^{3}\check{\Theta}_a\check{\mathcal{G}}_\epsilon\check{\Theta}_a.
\end{aligned} \tag{26}$$

It is easy to check that in the limit $\tau_s \to \infty$ this equation coincides with the corresponding equations in [23,37]. Note that the expression for $\check{\Gamma}_\epsilon$ has a nonzero Keldysh block which is not present in the case of potential disorder. We have to consider the solution of this equation for retarded, advanced, and Keldysh sub-blocks separately.

1. *Correction to the retarded and advanced Green's functions*

For the retarded and advanced blocks on the left-hand side of (25) we obtain

$$[\check{\Gamma}_\epsilon\check{g}_1(\epsilon, \epsilon') - \check{g}_1(\epsilon, \epsilon')\check{\Gamma}_{\epsilon'}]^{R(A)} = [(\zeta_\epsilon + \zeta_{\epsilon'})\hat{\mathcal{G}}_\epsilon\hat{g}_1(\epsilon, \epsilon')]^{R(A)}. \tag{27}$$

Here we introduce the functions

$$\zeta_\epsilon^R = \mathrm{sgn}(\epsilon)\tilde{\Delta}_\epsilon\sqrt{u_\epsilon^2 - 1}, \quad \zeta_\epsilon^A = -\left[\zeta_\epsilon^{(R)}\right]^* \tag{28}$$

because they allow us to simplify the resulting expressions by employing the normalization condition. It then follows that

$$\hat{g}_1^{R(A)}(\epsilon,\epsilon') = 2\pi\sum_{\nu\mu}\left[\frac{\hat{\mathcal{G}}_\epsilon\hat{\mathcal{R}}_Q(\epsilon,\epsilon') + \hat{\mathcal{G}}_\epsilon\hat{\mathcal{R}}_\Delta(\epsilon,\epsilon')}{\zeta_\epsilon + \zeta_{\epsilon'}}\right]^{R(A)} \times \delta(\epsilon' - \epsilon - \Omega_{\nu+\mu}). \quad (29)$$

We would like to note that, generally, Eq. (14) has two complex conjugate roots, so one needs to make sure that the root with the correct sign for the imaginary part is chosen such that the retarded function in (28) is analytic in the upper half plane of the complex variable $\tilde{\epsilon}$.

2. Correction to the Keldysh Green's function

Next, we need to compute a correction to the remaining (Keldysh) block. Correcting the Keldysh block of the Green's function is important since it determines the correction to the order parameter (6):

$$\Delta_1(t) = \frac{\pi\lambda}{2}\int\frac{d\epsilon}{2\pi}\int\frac{d\epsilon'}{2\pi}\mathrm{Tr}\{-\hat{\Xi}_2\hat{g}_1^K(\epsilon,\epsilon')\}e^{-i(\epsilon-\epsilon')t}. \quad (30)$$

The function $\hat{g}_1^K(\epsilon,\epsilon')$ is itself proportional to Δ_1, which will ultimately allow us to compute the pairing susceptibility. The frequency at which the susceptibility diverges determines the frequency of the amplitude (Higgs) mode ω_{Higgs}. Therefore, we will be able to directly verify whether ω_{Higgs} and 2Δ are equal to each other or not.

For the Keldysh component $\hat{g}_1^K(\epsilon,\epsilon')$ from (25) we find

$$\begin{aligned}\hat{N}_\epsilon^R\hat{g}_1^K(\epsilon,\epsilon') - \hat{g}_1^K(\epsilon,\epsilon')\hat{N}_{\epsilon'}^A &= 2\pi\sum_{\nu\mu}[\hat{\mathcal{R}}_Q^K(\epsilon,\epsilon') + \hat{\mathcal{R}}_\Delta^K(\epsilon,\epsilon')]\delta(\epsilon'-\epsilon-\Omega_{\nu+\mu})\\ &\quad + \hat{g}_1^R(\epsilon,\epsilon')\hat{\Lambda}_{\epsilon'}^K - \hat{\Lambda}_\epsilon^K\hat{g}_1^A(\epsilon,\epsilon'),\end{aligned} \quad (31)$$

where $\check{N}_\epsilon = \epsilon\check{\Xi}_3 + \check{\Delta}$ and $\check{\Lambda}_\epsilon = \check{\Gamma}_\epsilon - \check{N}_\epsilon$. The last two terms on the right-hand side of this equation appear explicitly due to scattering on paramagnetic impurities since $\hat{\Lambda}_\epsilon^K|_{\tau_s\to\infty} = 0$.

In order to solve (31) we again use the normalization condition (20), which for the Keldysh components reads

$$\hat{\mathcal{G}}_\epsilon^R\hat{g}_1^K(\epsilon,\epsilon') + \hat{\mathcal{G}}_\epsilon^K\hat{g}_1^A(\epsilon,\epsilon') + \hat{g}_1^R(\epsilon,\epsilon')\hat{\mathcal{G}}_{\epsilon'}^K + \hat{g}_1^K(\epsilon,\epsilon')\hat{\mathcal{G}}_{\epsilon'}^A = 0. \quad (32)$$

We look for the solution of Eq. (31) in the form

$$\hat{g}_1^K(\epsilon,\epsilon') = \hat{g}_{1,\mathrm{reg}}^K(\epsilon,\epsilon') + \hat{g}_{1,\mathrm{an}}^K(\epsilon,\epsilon'). \quad (33)$$

The first term, dubbed a regular term since it does not affect the single-particle distribution function in (33), is defined similarly to (9):

$$\hat{g}_{1,\mathrm{reg}}^K(\epsilon,\epsilon') = \hat{g}_1^R(\epsilon,\epsilon')n_{\epsilon'} - n_\epsilon\hat{g}_1^A(\epsilon,\epsilon'), \quad (34)$$

where we use the shorthand notation

$$n_\epsilon = \tanh\left(\frac{\epsilon}{2T}\right). \quad (35)$$

It is straightforward to verify that $\hat{g}_{1,\mathrm{reg}}^K(\epsilon,\epsilon')$ satisfies the normalization condition (32). As a result, it is clear that $\hat{g}_{1,\mathrm{an}}^K(\epsilon,\epsilon')$ must satisfy

$$\hat{\mathcal{G}}_\epsilon^R\hat{g}_{1,\mathrm{an}}^K(\epsilon,\epsilon') + \hat{g}_{1,\mathrm{an}}^K(\epsilon,\epsilon')\hat{\mathcal{G}}_{\epsilon'}^A = 0. \quad (36)$$

We now insert (33) into Eq. (31), and after some algebra (see Appendix A) we find

$$\hat{g}_{1,\mathrm{an}}^K(\epsilon,\epsilon') = 2\pi\sum_{\nu\mu}\frac{\hat{\rho}_Q(\epsilon,\epsilon') + \hat{\rho}_\Delta(\epsilon,\epsilon')}{\zeta_\epsilon^R + \zeta_{\epsilon'}^A}\delta(\epsilon'-\epsilon-\Omega_{\nu+\mu}). \quad (37)$$

The expressions for the matrix functions $\hat{\rho}_Q(\epsilon,\epsilon')$ and $\hat{\rho}_\Delta(\epsilon,\epsilon')$ are

$$\begin{aligned}\hat{\rho}_\Delta(\epsilon,\epsilon') &= [\hat{\mathcal{G}}_\epsilon^R\hat{\Delta}_1(\Omega_{\nu+\mu})\hat{\mathcal{G}}_{\epsilon'}^A - \hat{\Delta}_1(\Omega_{\nu+\mu})](n_{\epsilon'} - n_\epsilon),\\ \hat{\rho}_Q(\epsilon,\epsilon') &= iD[\hat{\mathcal{G}}_\epsilon^R\hat{\mathbf{Q}}_\nu\hat{\mathcal{G}}_{\epsilon+\Omega_\nu}^R\hat{\mathbf{Q}}_\mu\hat{\mathcal{G}}_{\epsilon'}^A - \hat{\mathbf{Q}}_\nu\hat{\mathcal{G}}_{\epsilon+\Omega_\nu}^R\hat{\mathbf{Q}}_\mu]\\ &\quad\times(n_{\epsilon'} - n_{\epsilon+\Omega_\nu})\\ &\quad - iD[\hat{\mathcal{G}}_\epsilon^R\hat{\mathbf{Q}}_\nu\hat{\mathcal{G}}_{\epsilon+\Omega_\nu}^A\hat{\mathbf{Q}}_\mu\hat{\mathcal{G}}_{\epsilon'}^A - \hat{\mathbf{Q}}_\nu\hat{\mathcal{G}}_{\epsilon+\Omega_\nu}^A\hat{\mathbf{Q}}_\mu]\\ &\quad\times(n_\epsilon - n_{\epsilon+\Omega_\nu}).\end{aligned} \quad (38)$$

Having computed $\hat{g}_1^K(\epsilon,\epsilon')$, we can directly insert it into the self-consistency equation and compute the resonant frequency of the amplitude Higgs mode.

III. AMPLITUDE HIGGS MODE

We will analyze the self-consistency Eq. (30), which contains two contributions:

$$\Delta_1(t) = \frac{\pi\lambda}{2}\int_{-\infty}^{\infty}\frac{d\epsilon}{2\pi}\int_{-\infty}^{\infty}\frac{d\epsilon'}{2\pi}\mathrm{Tr}\{(-\hat{\Xi}_2)[\hat{g}_{1,\mathrm{reg}}^K(\epsilon,\epsilon') + \hat{g}_{1,\mathrm{an}}^K(\epsilon,\epsilon')]\}e^{i(\epsilon'-\epsilon)t}. \quad (39)$$

Without loss of generality, here we consider the case when $\Omega_1 = 0$ and $\Omega_2 = \Omega$. This case is analogous to a setup in which a superconductor is prepared in a state which carries nonzero supercurrent. Thus, we will need to focus only on computing the Fourier component $\Delta_1(\Omega) = |\delta\Delta_\Omega|e^{i\Omega t}$. In the limit $\tau_s\to\infty$ the amplitude $|\delta\Delta_\Omega|$ has a maximum at $\Omega_{\mathrm{res}} = 2\Delta$, which corresponds to the excitation of the amplitude Higgs mode [23].

Using the expressions for the regular and anomalous contributions to the Keldysh component of the Green's functions from the previous section, the self-consistency equation for the Fourier component $\Delta_1(\Omega)$ can be cast in the following simple form:

$$\Delta_1(\Omega) = 2i\delta W_Q\left(\frac{B_{\mathrm{reg}}(\Omega) + B_{\mathrm{an}}(\Omega)}{A_{\mathrm{reg}}(\Omega) + A_{\mathrm{an}}(\Omega)}\right). \quad (40)$$

Here $\delta W_Q = D\mathbf{A}_0\mathbf{A}_\Omega$. Functions $A_{\mathrm{reg}}(\Omega)$ and $A_{\mathrm{an}}(\Omega)$ are defined according to

$$\begin{aligned}A_{\mathrm{reg}}(\Omega) &= \int_{-\infty}^{\infty}d\epsilon\left(\frac{1 + g_\epsilon^Rg_{\epsilon+\Omega}^R + f_\epsilon^Rf_{\epsilon+\Omega}^R}{\zeta_\epsilon^R + \zeta_{\epsilon+\Omega}^R}\right)n_{\epsilon+\Omega}\\ &\quad - \int_{-\infty}^{\infty}d\epsilon\left(\frac{1 + g_\epsilon^Ag_{\epsilon+\Omega}^A + f_\epsilon^Af_{\epsilon+\Omega}^A}{\zeta_\epsilon^A + \zeta_{\epsilon+\Omega}^A} - \frac{f_\epsilon^R - f_\epsilon^A}{\Delta}\right)n_\epsilon,\\ A_{\mathrm{an}}(\Omega) &= \int_{-\infty}^{\infty}\frac{(n_\epsilon - n_{\epsilon+\Omega})}{\zeta_\epsilon^R + \zeta_{\epsilon+\Omega}^A}(1 + g_\epsilon^Rg_{\epsilon+\Omega}^A + f_\epsilon^Rf_{\epsilon+\Omega}^A)d\epsilon.\end{aligned} \quad (41)$$

The term $\propto(f_\epsilon^R - f_\epsilon^A)$ in the expression for $A_{\mathrm{reg}}(\Omega)$ replaces the contribution from $1/\lambda$ by virtue of the self-consistency condition at equilibrium. The expression for $A_{\rm an}(\Omega)$ involves a combination of retarded and advanced Green's functions and therefore has poles in both the upper and lower half planes of the complex variable ϵ. That is not so for $A_{\rm reg}(\Omega)$, in which all contributions containing retarded and advanced functions can be separated from each other. Therefore, in the expression for $A_{\rm reg}(\Omega)$ we can reduce the integration over ϵ to the summation over the fermionic Matsubara frequencies $\omega_l = \pi T(2l+1)\,(l = 0, \pm 1, \dots)$ by using the series representation $\tanh x = \sum_l 2x/[\pi^2(l+1/2)^2 + x^2]$. Subsequent integration in the upper or lower complex half plane with respect to complex ϵ then yields

$$\int_{-\infty}^{\infty} G^{R(A)}(\epsilon)\tanh\left(\frac{\epsilon}{2T}\right)d\epsilon = \pm 4\pi i T\sum_{l=0}^{\infty} G(\pm i\omega_l). \quad (42)$$

The corresponding expressions for the Green's functions are listed in Appendix B.

Last, we also find the following expressions for functions $B_{\rm reg}(\Omega)$ and $B_{\rm an}(\Omega)$:

$$B_{\rm reg}(\Omega) = \int_{-\infty}^{\infty} d\epsilon\left(\frac{g_\epsilon^R + g_{\epsilon+\Omega}^R}{\zeta_\epsilon^R + \zeta_{\epsilon+\Omega}^R}\right)\left(g_\epsilon^R f_{\epsilon+\Omega}^R + f_\epsilon^R g_{\epsilon+\Omega}^R\right)n_{\epsilon+\Omega} - \int_{-\infty}^{\infty} d\epsilon\left(\frac{g_\epsilon^A + g_{\epsilon+\Omega}^A}{\zeta_\epsilon^A + \zeta_{\epsilon+\Omega}^A}\right)\left(g_\epsilon^A f_{\epsilon+\Omega}^A + f_\epsilon^A g_{\epsilon+\Omega}^A\right)n_\epsilon,$$

$$B_{\rm an}(\Omega) = \int_{-\infty}^{\infty} d\epsilon\frac{(n_\epsilon - n_{\epsilon+\Omega})}{\zeta_\epsilon^R + \zeta_{\epsilon+\Omega}^A}\left(g_\epsilon^R + g_{\epsilon+\Omega}^A\right) \times \left(g_\epsilon^R f_{\epsilon+\Omega}^A + f_\epsilon^R g_{\epsilon+\Omega}^A\right). \quad (43)$$

As discussed above, in order to compute the frequency dependence of $B_{\rm reg}(\Omega)$ we convert the integral over ϵ into the summation over the fermionic Matsubara frequencies. In passing we note that expressions (41) and (43) match the corresponding formulas in Refs. [23,37], and therefore, we expect to recover their results in the limit $\zeta \to 0$. The results of the numerical calculation of the frequency dependence of functions $A_{\rm reg}(\Omega) + A_{\rm an}(\Omega)$ and $B_{\rm reg}(\Omega) + B_{\rm an}(\Omega)$ are given in Figs. 6 and 7 in Appendix B.

Having computed these functions, we can now compute the amplitude of the resonant Higgs mode using Eq. (40). The results of the numerical calculation are presented in Fig. 2. We immediately observe that with a small increase in the strength of magnetic scattering, the frequency of the resonant mode moves to the left, i.e., $\Omega_{\rm res}(\zeta \neq 0) < 2\Delta$. This result qualitatively agrees with that of Ref. [57]. We also see that the amplitude mode $|\Delta_1(\Omega)|$ decreases with an increase in ζ. This result goes beyond the perturbative one of Ref. [57], where the amplitude of the periodic oscillations was proportional to ζ. Therefore, we expect that the amplitude Higgs mode will be significantly suppressed before the gapless state is reached. The importance of our result $\Omega_{\rm res} < 2\Delta$ lies in the fact that, according to Ref. [57], in this case the dynamics of the amplitude mode becomes dissipationless; i.e., $\Delta_1(t)$ will periodically vary in time on a timescale $t \ll \tau_{\text{e-e}}$. In order to show this explicitly within the confines of the present theoretical framework, we will have to determine the dynamics of the order parameter by solving the Usadel equation using (19) as an initial condition. This is an arduous task which we leave for future studies.

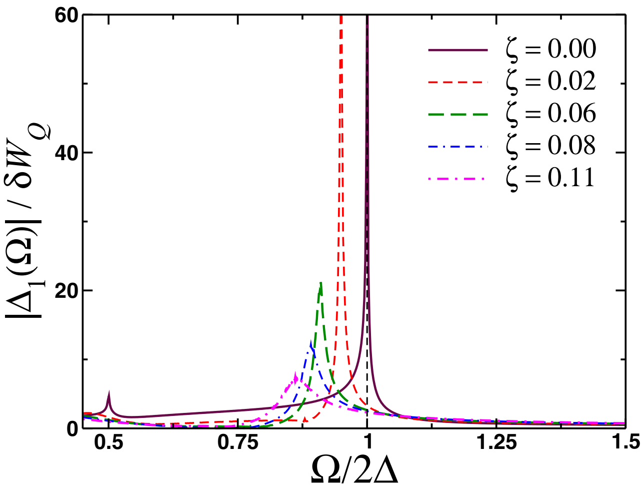

FIG. 2. Frequency dependence of the amplitude mode $\Delta_1(\Omega)$. The frequency Ω is shown in units of the pairing amplitude Δ for various values of the dimensionless parameter $\zeta = 1/\tau_s\Delta$. The amplitude mode has a maximum for $\zeta = 0$ at $\Omega_{\rm res} = 2\Delta$. As we increase the value of the magnetic disorder parameter ζ the value of the resonant frequency shifts below 2Δ. Note that the amplitude of the resonant Higgs mode decreases with increasing strength of the magnetic disorder.

IV. CURRENT INDUCED BY AN EXTERNAL ELECTROMAGNETIC FIELD

In this section we discuss the current induced by external electromagnetic radiation. Our main motivation is to get insight into the origin of the shift in the resonance frequency from its value 2Δ in a disordered superconductor without magnetic impurities. We consider a time-dependent external electric field

$$\mathbf{E}(t) = \mathbf{E}_\Omega\cos(\Omega t) + \mathbf{E}_{\omega_{\rm p}}\cos(\omega_{\rm p} t). \quad (44)$$

The first term here describes the "pump field" $\mathbf{E}_\Omega$, while the second one is the "probe field" $\mathbf{E}_{\omega_{\rm p}}$. The vector potential $\mathbf{A}(t)$ has the same form as (44), with the corresponding Fourier components given by

$$\mathbf{A}_\Omega = -\frac{i\mathbf{E}_\Omega}{\Omega}, \quad \mathbf{A}_\omega = -\frac{i\mathbf{E}_\omega}{\omega}. \quad (45)$$

Here we use the units $\hbar = e = c = 1$. The expression for the electric current can be compactly written as

$$\mathbf{j}(\omega) = -\mathcal{Q}(\omega, \omega')\mathbf{A}_{\omega'}, \quad (46)$$

where $\mathcal{Q}(\omega, \omega')$ is the response kernel (we refer the reader to Appendix C for details):

$$\mathcal{Q}(\omega, \omega') = \frac{\pi\sigma_D}{4i}\int_{-\infty}^{\infty}\frac{d\epsilon}{2\pi}\int_{-\infty}^{\infty}\frac{d\epsilon'}{2\pi} \times {\rm Tr}\{\hat{\Xi}_3\hat{G}^R(\epsilon, \epsilon' - \omega')\hat{\Xi}_3\hat{G}^K(\epsilon', \epsilon + \omega) + \hat{G}^K(\epsilon, \epsilon' - \omega')\hat{\Xi}_3\hat{G}^A(\epsilon', \epsilon + \omega)\hat{\Xi}_3\}. \quad (47)$$

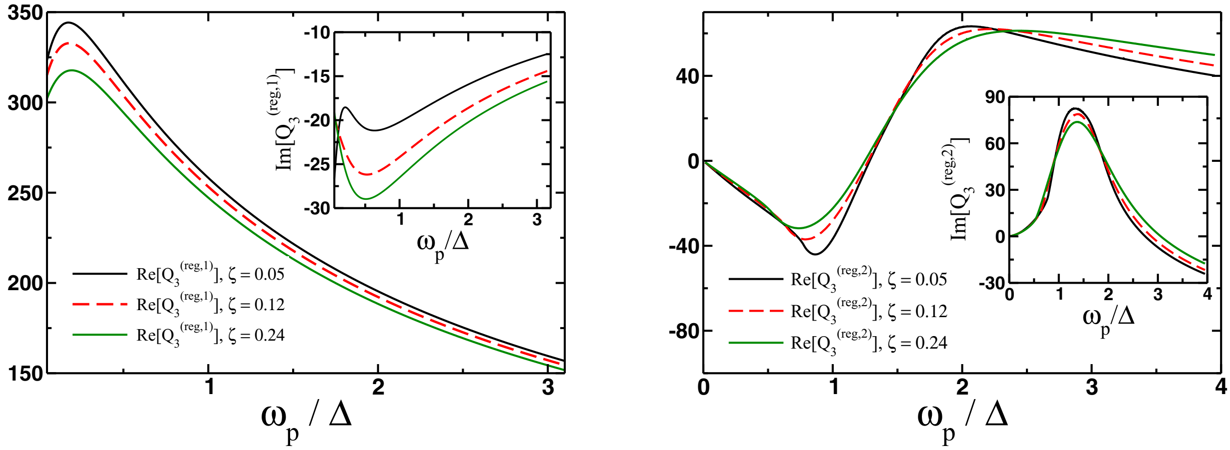

FIG. 3. Plots of the real (main plot) and imaginary (inset) parts of the functions $\mathcal{Q}_3^{(\mathrm{reg1})}(\Omega,\omega_\mathrm{p})$ (left panel) and $\mathcal{Q}_3^{(\mathrm{reg2})}(\Omega,\omega_\mathrm{p})$ (right panel) as a function of the probe frequency with the value of the pump frequency fixed to $\Omega = 0.895\Delta$ for various values of the dimensionless parameter ζ. Note that for the wide range of frequencies $|\mathcal{Q}_3^{(\mathrm{reg1})}| \gg |\mathcal{Q}_3^{(\mathrm{reg2})}|$. Both functions are given in units of $\delta W_Q \sigma_D$.

It is straightforward to verify that in the limit of very weak electromagnetic field we recover the familiar expression for the current [62].

A. Third harmonic term in the current

We are mainly interested in the calculation of the third harmonic. One would generally expect the third harmonic component of the kernel to display a feature (e.g., a cusp) at $\omega_\mathrm{p} = \Delta$, and we are interested in whether this feature remains at Δ or shifts below Δ, similar to the resonance frequency Ω_res discussed above.

The response kernel for the third harmonic must be of the order of $O(A^2)$. It is convenient to write it as the sum of three terms:

$$\mathcal{Q}_3 = \mathcal{Q}_3^{(\mathrm{an})} + \mathcal{Q}_3^{(\mathrm{reg1})} + \mathcal{Q}_3^{(\mathrm{reg2})}. \tag{48}$$

Here the first term is the anomalous one defined by $\hat{g}_{1,\mathrm{an}}^K$, and it describes the effects associated with the nonequilibrium effects on the distribution function:

$$\mathcal{Q}_3^{(\mathrm{an})}(\omega,\omega') = \frac{\sigma_D}{8i}\int_{-\infty}^{\infty} \mathrm{Tr}\{\hat{g}_{1,\mathrm{an}}^K(E, E+\omega-\omega') \times (\hat{\mathcal{G}}_{E-\omega'}^R + \hat{\mathcal{G}}_{E+\omega}^A)\} dE. \tag{49}$$

The remaining two terms can be classified as regular terms since they involve the distribution functions in equilibrium:

$$\begin{aligned}
\mathcal{Q}_3^{(\mathrm{reg1})}(\omega,\omega') &= \frac{\sigma_D}{8i}\int_{-\infty}^{\infty} \mathrm{Tr}\{\hat{g}_1^R(E, E+\omega-\omega')[\hat{\mathcal{G}}_{E-\omega'}^R n_{E+\omega-\omega'} + \hat{\mathcal{G}}_{E+\omega}^R n_{E+\omega}]\} dE \\
&\quad - \frac{\sigma_D}{8i}\int_{-\infty}^{\infty} \mathrm{Tr}\{\hat{g}_1^A(E, E+\omega-\omega')[\hat{\mathcal{G}}_{E-\omega'}^A n_{E-\omega'} + \hat{\mathcal{G}}_{E+\omega}^A n_E]\} dE, \\
\mathcal{Q}_3^{(\mathrm{reg2})}(\omega,\omega') &= \frac{\sigma_D}{8i}\int_{-\infty}^{\infty} \mathrm{Tr}\{\hat{g}_1^R(E, E+\omega-\omega')\hat{\mathcal{G}}_{E+\omega}^A\}(n_{E+\omega-\omega'} - n_{E+\omega}) dE \\
&\quad + \frac{\sigma_D}{8i}\int_{-\infty}^{\infty} \mathrm{Tr}\{\hat{g}_1^A(E, E+\omega-\omega')\hat{\mathcal{G}}_{E-\omega'}^R\}(n_E - n_{E-\omega'}) dE.
\end{aligned} \tag{50}$$

We would like to remind the reader that n_E, Eq. (35), is not a single-particle Fermi distribution function; however, it is related to it by $n_E = 1 - 2n_F(E)$. The reason for considering two terms in (50) separately is purely technical: The integral over energies in $\mathcal{Q}_3^{(\mathrm{reg1})}$ can be converted into the summations over the fermionic Matsubara frequencies just like what was been done in the calculation of $\Delta_1(\Omega)$. Hence, we expect that this function will exhibit monotonic behavior as a function of ω' for fixed ω.

We first proceed with the numerical calculation of the kernel $\mathcal{Q}_3$. In expressions (38) we set $\Omega_\nu = \Omega_\mu = \Omega$ and $\Omega_{\nu+\mu} = 2\Omega$. This implies that $\hat{g}_{1,\mathrm{an}}^K$ is nonzero provided $\omega - \omega' = 2\Omega$. Since, by definition, $\omega' = \omega_\mathrm{p}$ [see Eq. (46)], it follows that $\omega = 2\Omega + \omega_\mathrm{p}$. We evaluate the dependence of $\mathcal{Q}_3^{(\mathrm{an})}$, $\mathcal{Q}_3^{(\mathrm{reg1})}$, and $\mathcal{Q}_3^{(\mathrm{reg2})}$ on the probe frequency ω_p at low temperatures $T = 10^{-5}\Delta$ and for $\Omega \sim \Delta$. The dependence of the complex functions $\mathcal{Q}_3^{(\mathrm{reg1})}$ and $\mathcal{Q}_3^{(\mathrm{reg2})}$ on the probe frequency is shown in Fig. 3, and the dependence of $\mathcal{Q}_3^{(\mathrm{an})}$ is presented in Fig. 4. Interestingly, we also observe that the real part of $\mathcal{Q}_3^{(\mathrm{reg1})}$ significantly exceeds that of $\mathcal{Q}_3^{(\mathrm{reg2})}$, while the imaginary parts are comparable to each other. This observation confirms our earlier expectations that the dominant contribution to both of these functions comes from the terms proportional to Δ_1 [37].

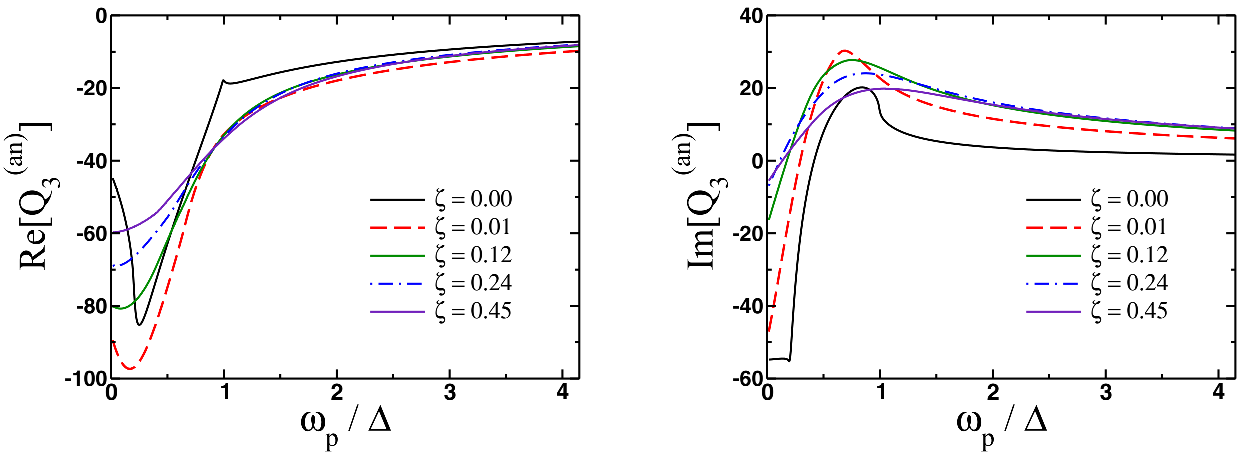

FIG. 4. Plots of the real (left panel) and imaginary (right panel) parts of the function $\mathcal{Q}_3^{(\mathrm{an})}(\Omega, \omega_\mathrm{p})$ as a function of the probe frequency ω_p for several values of the dimensionless parameter ζ. The value of the pump frequency is fixed to $\Omega = 0.895\Delta$. Both functions are given in units of $\delta W_Q \sigma_D$. For both plots we set $\Delta_1(2\Omega) = 12\delta W_Q$.

In addition, we observe a cusplike feature in the dependence of $\mathrm{Re}[\mathcal{Q}_3^{(\mathrm{an})}]$ (and a "weak discontinuity" in $\mathrm{Im}[\mathcal{Q}_3^{(\mathrm{an})}]$) at $\omega_\mathrm{p} \approx \Delta$ for $\zeta = 0$, which shifts to smaller values and is almost completely smeared away at larger values of ζ (Fig. 4). A more detailed analysis of the third harmonic contribution to the current will be carried out when the experimental data become available.

V. DISCUSSION

Our main finding—the reduction of the resonance frequency Ω_res below 2Δ—requires further discussion. At first glance it seems that the decrease in the resonance frequency (Figs. 2 and 5) and the qualitatively similar finding in Ref. [57] for the frequency of the Higgs mode $\omega_\mathrm{Higgs} = 2\Delta\sqrt{1-\zeta^2}$ emerge from the mathematics. We believe, however, that the approach we used in this paper allows us to give a clear physical interpretation of this result. Our calculation for the third harmonic of the electric current can be used to give a more intuitive interpretation of the reduction in Ω_res. We first recall that in diffusive superconductors even in the absence of magnetic disorder the third harmonic generating current is mostly dominated by the amplitude Higgs mode [37]. We recall also that in the linear approximation the superfluid stiffness is directly proportional to the pairing amplitude and with an increase of magnetic scattering it decreases more slowly than the single-particle threshold energy (Fig. 5). Therefore, we are led to conclude that the nonlinear suppression of the superfluid stiffness and the reduction in the frequency of the amplitude Higgs mode are two correlated effects; i.e., the reduction of the superfluid stiffness through the nonlinear coupling to the external electromagnetic field is reflected in the decrease of the resonant frequency. In this regard we suggest that in addition to the two energy scales $\Delta_\mathrm{th}(\zeta)$ and $\Delta(\zeta)$, for a complete description of a conventional superconductor with weak magnetic impurities we need to consider an additional energy scale, $\Omega_\mathrm{res}(\zeta)$. Last, we mention that a similar effect, the reduction of the frequency of the amplitude Higgs mode below 2Δ, was discussed for various situations [68,72] which are manifestly different from our mechanism, so the underlying physical processes responsible for this reduction are most likely different as well.

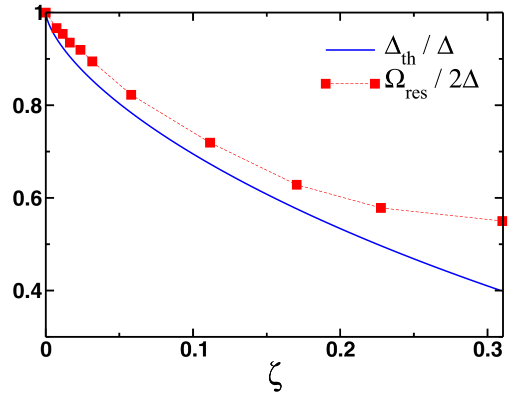

FIG. 5. The dependence of the single-particle threshold energy $\Delta_\mathrm{th} = \Delta(1-\zeta^{2/3})^{3/2}$ and the resonant frequency of the amplitude Higgs mode Ω_res in units of 2Δ. The frequency of the resonance mode remains above the single-particle threshold energy but below the pair excitation energy 2Δ. In the regime of collisionless dynamics these results imply that the dynamics of the amplitude mode remains dissipationless on a timescale much shorter than the timescale for the two-particle collisions.

However, we also have to mention that the dependence of Ω_res on ζ does not match that of ω_Higgs on ζ. The origin of this discrepancy is not clear to us at this point. In order to gain further insight we will have to compute the time dependence of the pairing amplitude $\Delta(t)$ after the electromagnetic pulse by directly solving the Usadel equation (4). From the form of the Usadel equation it is clear that the magnetic impurities do not lead to relaxation; therefore, we will need to check only if the magnetic impurities lead to the suppression of the dephasing processes which render the order parameter dynamics dissipationless. Given the fact that scattering on magnetic impurities leads to the smearing of the square-root singularity in the single particle density of states (Fig. 1), it is indeed likely that the dynamics of the amplitude mode will exhibit periodic oscillations. Last, we limited our discussion to the self-consistent Born approximation and did not consider the bound states which form on magnetic impurities. On a technical level, this requires a modification of the Usadel equation [62,73,74]. We will consider the effects associated with the bound states, including the dynamics of the pairing amplitude and third harmonic of the current, in a separate publication.

VI. CONCLUSIONS

We considered a problem of the nonlinear response of conventional (BCS) superconductors contaminated by weak magnetic impurities to the external time-dependent electromagnetic field. Specifically, we computed the resonant frequency of the amplitude mode and third harmonic contribution to the electric current. Our main result is that the resonant frequency remains below the pair excitation threshold 2Δ with an increase in scattering due to magnetic disorder. We attribute this shift to the nonlinear suppression of the superfluid density. Taken together with the results of Ref. [57], our present findings unambiguously suggest that the dynamics of the pairing amplitude should remain periodic in time. We also found that with an increase in magnetic scattering the third harmonic is suppressed along with the amplitude of the resonant mode. We attribute this effect to the nonlinear suppression of the superfluid density.

ACKNOWLEDGMENTS

We would like to thank M. Khodas, A. Levchenko, and D. Pesin for their interest in this work and useful discussions. We gratefully acknowledge the financial support from the National Science Foundation Grant No. DMR-2002795 (Y.L. and M.D.). This project was started during the Aspen Center of Physics 2023 Summer Program on "New Directions on Strange Metals in Correlated Systems," which was supported by the National Science Foundation, Grant No. PHY-2210452.

APPENDIX A: DERIVATION OF THE EXPRESSION FOR $\hat{g}^K_{1,\mathrm{an}}(\epsilon,\epsilon')$

In this Appendix we provide the details of the derivation of Eq. (37) in the main text. Our starting point is Eq. (31). Let us first consider only terms which contain $\hat{g}^K_{1,\mathrm{reg}}(\epsilon,\epsilon')$:

$$\begin{aligned}\hat{N}^R_\epsilon \hat{g}^K_{1,\mathrm{reg}}(\epsilon,\epsilon') - \hat{g}^K_{1,\mathrm{reg}}(\epsilon,\epsilon')\hat{N}^A_{\epsilon'} &= \big(\hat{N}^R_\epsilon \hat{g}^R_1 - \hat{g}^R_1\hat{N}^A_{\epsilon'}\big)n_{\epsilon'} - n_\epsilon\big(\hat{N}^R_\epsilon \hat{g}^A_1 - \hat{g}^A_1\hat{N}^A_{\epsilon'}\big)\\ &= \big(\hat{N}^R_\epsilon \hat{g}^R_1 - \hat{g}^R_1\hat{N}^R_{\epsilon'}\big)n_{\epsilon'} - n_\epsilon\big(\hat{N}^A_\epsilon \hat{g}^A_1 - \hat{g}^A_1\hat{N}^A_{\epsilon'}\big) + g^R_1\big(\hat{N}^R_{\epsilon'} - \hat{N}^A_{\epsilon'}\big)n_{\epsilon'} - n_\epsilon\big(\hat{N}^R_\epsilon - \hat{N}^A_\epsilon\big)g^A_1.\end{aligned} \tag{A1}$$

If we now look at Eq. (25), we note that $\check{\Lambda}_\epsilon$ has only a nonzero Keldysh component. We have

$$\begin{aligned}&\big(\hat{N}^R_\epsilon \hat{g}^R_1 - \hat{g}^R_1\hat{N}^R_{\epsilon'}\big)n_{\epsilon'} - n_\epsilon\big(\hat{N}^A_\epsilon \hat{g}^A_1 - \hat{g}^A_1\hat{N}^A_{\epsilon'}\big)\\ &\quad= 2\pi\sum_{\nu\mu}\big[\hat{\mathcal{R}}^R_Q(\epsilon,\epsilon')n_{\epsilon'} - n_\epsilon\hat{\mathcal{R}}^A_Q(\epsilon,\epsilon') + \hat{\mathcal{R}}^R_\Delta(\epsilon,\epsilon')n_{\epsilon'} - n_\epsilon\hat{\mathcal{R}}^A_\Delta(\epsilon,\epsilon')\big]\delta(\epsilon'-\epsilon-\Omega_{\nu+\mu})\\ &\quad\equiv \hat{\mathcal{P}}^R(\epsilon,\epsilon')n_{\epsilon'} - n_\epsilon\hat{\mathcal{P}}^A(\epsilon,\epsilon').\end{aligned} \tag{A2}$$

Here $\hat{\mathcal{P}}^{R(A)}(\epsilon,\epsilon')$ are used to keep the expressions as compact as possible. Let us now consider the remaining two terms in (A1):

$$\begin{aligned}&\hat{g}^R_1(\epsilon,\epsilon')\big(\hat{N}^R_{\epsilon'} - \hat{N}^A_{\epsilon'}\big)n_{\epsilon'} - n_\epsilon\big(\hat{N}^R_\epsilon - \hat{N}^A_\epsilon\big)\hat{g}^A_1(\epsilon,\epsilon')\\ &\quad= \hat{g}^R_1(\epsilon,\epsilon')\big[\big(g^R_{\epsilon'} - g^A_{\epsilon'}\big)\hat{\Xi}_3 - \big(f^R_{\epsilon'} - f^A_{\epsilon'}\big)\hat{\Xi}_2\big]\frac{in_{\epsilon'}}{2\tau_s} - \frac{in_\epsilon}{2\tau_s}\big[\big(g^R_\epsilon - g^A_\epsilon\big)\hat{\Xi}_3 - \big(f^R_\epsilon - f^A_\epsilon\big)\hat{\Xi}_2\big]\hat{g}^A_1(\epsilon,\epsilon')\\ &\quad= \hat{g}^R_1(\epsilon,\epsilon')\hat{\Lambda}^K_{\epsilon'} - \hat{\Lambda}^K_\epsilon\hat{g}^A_1(\epsilon,\epsilon'),\end{aligned} \tag{A3}$$

where we take into account formula (9) in the main text. Therefore, we find that

$$\hat{N}^R_\epsilon \hat{g}^K_{1,\mathrm{reg}}(\epsilon,\epsilon') - \hat{g}^K_{1,\mathrm{reg}}(\epsilon,\epsilon')\hat{N}^A_{\epsilon'} = \hat{\mathcal{P}}^R(\epsilon,\epsilon')n_{\epsilon'} - n_\epsilon\hat{\mathcal{P}}^A(\epsilon,\epsilon') + \hat{g}^R_1(\epsilon,\epsilon')\hat{\Lambda}^K_{\epsilon'} - \hat{\Lambda}^K_\epsilon\hat{g}^A_1(\epsilon,\epsilon'). \tag{A4}$$

We now insert this expression into Eq. (31). The terms which contain $\check{\Lambda}_\epsilon$ cancel out, and we obtain

$$\hat{N}^R_\epsilon \hat{g}^K_{1,\mathrm{an}}(\epsilon,\epsilon') - \hat{g}^K_{1,\mathrm{an}}(\epsilon,\epsilon')\hat{N}^A_{\epsilon'} = \hat{\mathcal{P}}^K(\epsilon,\epsilon') - \hat{\mathcal{P}}^R(\epsilon,\epsilon')n_{\epsilon'} + n_\epsilon\hat{\mathcal{P}}^A(\epsilon,\epsilon'). \tag{A5}$$

Interestingly, this equation has the same form as the one for the case of nonmagnetic disorder. Let us now simplify the expression on the right-hand side of Eq. (A5):

$$\hat{\mathcal{P}}^K_\Delta(\epsilon,\epsilon') - \hat{\mathcal{P}}^R_\Delta(\epsilon,\epsilon')n_{\epsilon'} + n_\epsilon\hat{\mathcal{P}}^A_\Delta(\epsilon,\epsilon') = 2\pi\sum_{\nu\mu}(n_\epsilon - n_{\epsilon'})\big[\hat{\mathcal{G}}^R_\epsilon\hat{\Delta}_1(\Omega_{\nu+\mu}) - \hat{\Delta}_1(\Omega_{\nu+\mu})\hat{\mathcal{G}}^A_{\epsilon'}\big]\delta(\epsilon'-\epsilon-\Omega_{\nu+\mu}). \tag{A6}$$

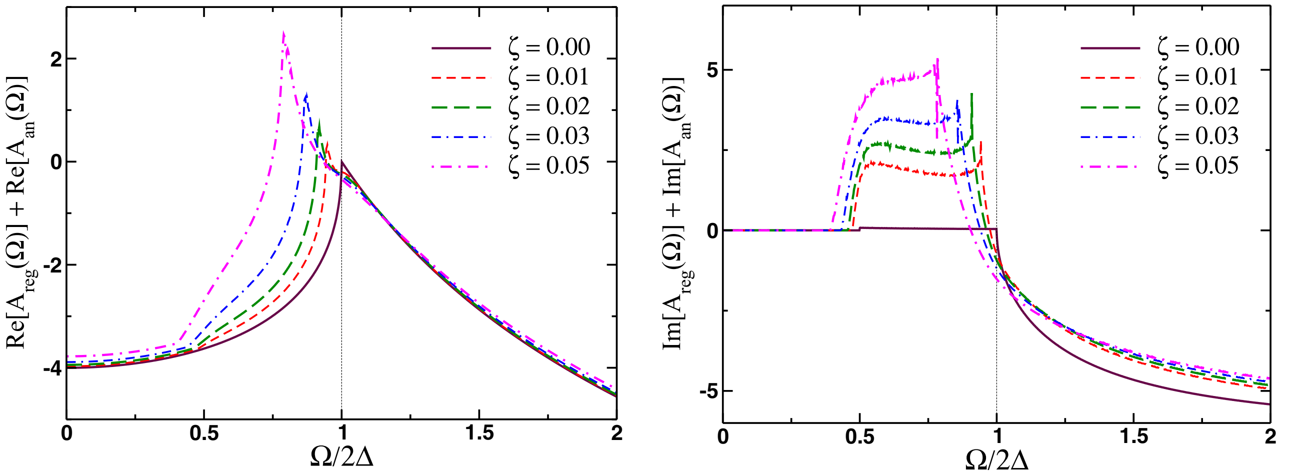

FIG. 6. Frequency dependence of the real and imaginary parts of the function $A(\Omega) = A_{\text{reg}}(\Omega) + A_{\text{an}}(\Omega)$. The frequency is shown in units of the pairing amplitude Δ for various values of the dimensionless parameter $\zeta = 1/\tau_s\Delta$.

In passing we note that this result matches the corresponding expressions in Refs. [23,37]. For the remaining contribution we find

$$\begin{aligned}\hat{\mathcal{P}}_Q^K(\epsilon,\epsilon') - \hat{\mathcal{P}}_Q^R(\epsilon,\epsilon')n_{\epsilon'} + n_\epsilon \hat{\mathcal{P}}_Q^A(\epsilon,\epsilon') &= 2\pi i D\sum_{\nu\mu}\big[\hat{\mathbf{Q}}_\nu \hat{\mathcal{G}}^R_{\epsilon+\Omega_\nu}\hat{\mathbf{Q}}_\mu \hat{\mathcal{G}}^A_{\epsilon'} - \hat{\mathcal{G}}^R_\epsilon \hat{\mathbf{Q}}_\nu \hat{\mathcal{G}}^R_{\epsilon+\Omega_\nu}\hat{\mathbf{Q}}_\mu\big](n_{\epsilon'}-n_{\epsilon+\Omega_\nu})\delta(\epsilon'-\epsilon-\Omega_{\nu+\mu}) \\ &\quad - 2\pi i D\sum_{\nu\mu}\big[\hat{\mathbf{Q}}_\nu \hat{\mathcal{G}}^A_{\epsilon+\Omega_\nu}\hat{\mathbf{Q}}_\mu \hat{\mathcal{G}}^A_{\epsilon'} - \hat{\mathcal{G}}^R_\epsilon \hat{\mathbf{Q}}_\nu \hat{\mathcal{G}}^A_{\epsilon+\Omega_\nu}\hat{\mathbf{Q}}_\mu\big](n_{\epsilon}-n_{\epsilon+\Omega_\nu})\delta(\epsilon'-\epsilon-\Omega_{\nu+\mu}),\end{aligned} \tag{A7}$$

which is also in agreement with the results of Refs. [23,37]. Finally, we represent

$$\hat{N}^R_\epsilon \hat{g}^K_{1,\text{an}}(\epsilon,\epsilon') - \hat{g}^K_{1,\text{an}}(\epsilon,\epsilon')\hat{N}^A_{\epsilon'} = \big(\zeta^R_\epsilon + \zeta^A_{\epsilon'}\big)\hat{\mathcal{G}}^R_\epsilon \hat{g}^K_1(\epsilon,\epsilon') \tag{A8}$$

and solve the resulting equation for $\hat{g}^K_{1,\text{an}}(\epsilon,\epsilon')$ by employing the normalization condition. This yields (37) in the main text.

APPENDIX B: GREEN'S FUNCTIONS IN THE MATSUBARA REPRESENTATION

In this Appendix we provide the expressions for the Green's functions in the Matsubara representation. After making the substitution $\epsilon \to i\omega_l$, it follows that $g^{R(A)}_\epsilon \to g_{\omega_l}$, $g^{R(A)}_{\epsilon+\Omega} \to g_{\omega_l - i\Omega}$, $f^{R(A)}_\epsilon \to i f_{i\omega_l}$, and $f^{R(A)}_{\epsilon+\Omega} \to i f_{\omega_l - i\Omega}$. Introducing

$$\tilde{\omega}_l = \omega_l + \frac{g_{\omega_l}}{2\tau_s}, \quad \tilde{\Delta}_l = \Delta - \frac{f_{\omega_l}}{2\tau_s}, \tag{B1}$$

and $u_{\omega_l} = \tilde{\omega}_l/\tilde{\Delta}_l$, from the normalization condition $g^2_{\omega_l} + f^2_{\omega_l} = 1$ we find $g_{\omega_l} = u_{\omega_l}/\sqrt{u^2_{\omega_l}+1}$ and $f_{\omega_l} = 1/\sqrt{u^2_{\omega_l}+1}$. The function u_{ω_l} is found by solving the nonlinear equation [58]:

$$\left(1 - \frac{1}{\tau_s\Delta}\frac{1}{\sqrt{u^2_{\omega_l}+1}}\right)u_{\omega_l} = \frac{\omega_l}{\Delta}. \tag{B2}$$

We note that $u_{\omega_l} = -u_{-\omega_l}$. Using this property, we can now cast the expressions for functions $A_{\text{reg}}(\Omega)$ and $B_{\text{reg}}(\Omega)$ into the following form:

$$A_{\text{reg}}(\Omega) = 8\pi T\sum_{l=0}^{\infty}\left(\frac{1 + g_{\omega_l}g_{\omega_l+i\Omega} - f_{\omega_l}f_{\omega_l+i\Omega}}{\zeta_{\omega_l}+\zeta_{\omega_l+i\Omega}} - \frac{f_{\omega_l}}{\Delta}\right), \quad B_{\text{reg}}(\Omega) = 8\pi i T\sum_{l=0}^{\infty}\left(\frac{g_{\omega_l}+g_{\omega_l+i\Omega}}{\zeta_{\omega_l}+\zeta_{\omega_l+i\Omega}}\right)(g_{\omega_l}f_{\omega_l+i\Omega} + f_{\omega_l}g_{\omega_l+i\Omega}). \tag{B3}$$

When temperatures are close to absolute zero, we can convert the summation over l to integration:

$$2\pi T\sum_{l=0}^{\infty} \to \int_0^\infty d\omega_l. \tag{B4}$$

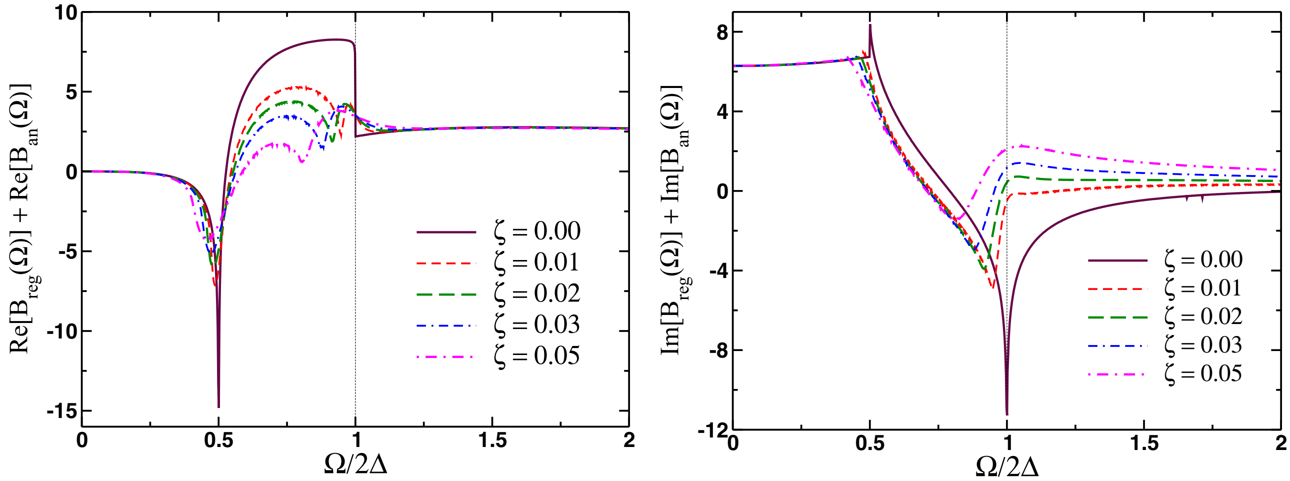

FIG. 7. Frequency dependence of the real and imaginary parts of the function $B(\Omega) = B_{\mathrm{reg}}(\Omega) + B_{\mathrm{an}}(\Omega)$. The frequency is shown in units of the pairing amplitude Δ for various values of the dimensionless parameter $\zeta = 1/\tau_s\Delta$.

The results of the numerical calculations of functions $A_{\mathrm{reg}}(\Omega)$ and $B_{\mathrm{reg}}(\Omega)$ are shown in Figs. 6 and 7. Note that the cusplike feature when $\zeta = 0$ in both the real and imaginary parts at $\Omega \approx 2\Delta$ moves to smaller values of $\Omega/2\Delta$ with an increase in the values of ζ.

APPENDIX C: ELECTROMAGNETIC FIELD RESPONSE KERNEL

The expression for the current can be derived from the same effective action of the nonlinear σ model which was used to derive the Usadel equation (4). Following the path of Refs. [70,71] by varying the corresponding part of the effective action with respect to the quantum component of the gradient vector potential $\mathbf{A}^{(q)}(t)$ for the electric current, we find

$$\mathbf{j}(t) = \frac{i\pi\sigma_D}{4}\int_{-\infty}^{\infty} dt_1 \mathrm{Tr}\{\hat{G}^R(t,t_1)\hat{\tilde{G}}^K(t_1,t) + \hat{G}^K(t,t_1)\hat{\tilde{G}}^A(t_1,t)\}\mathbf{A}(t_1). \tag{C1}$$

Here we introduce the compact notation $\hat{\tilde{G}}(t,t') = \hat{\Xi}_3\hat{G}(t,t')\hat{\Xi}_3$, $\sigma_D = 2e^2\nu_0 D$ is the Drude conductivity, and at the intermediate stages of the calculation we use the normalization condition (5). Performing the Fourier transformation in (C1) yields

$$\mathbf{j}(\omega) = -\mathcal{Q}(\omega,\omega')\mathbf{A}_{\omega'}, \tag{C2}$$

where the kernel $\mathcal{Q}(\omega,\omega')$ is determined from

$$\mathcal{Q}(\omega,\omega') = \frac{\pi\sigma_D}{4i}\int_{-\infty}^{\infty}\frac{d\epsilon}{2\pi}\int_{-\infty}^{\infty}\frac{d\epsilon'}{2\pi}\mathrm{Tr}\{\hat{\tilde{G}}^R(\epsilon,\epsilon'-\omega')\hat{G}^K(\epsilon',\epsilon+\omega) + \hat{G}^K(\epsilon,\epsilon'-\omega')\hat{\tilde{G}}^A(\epsilon',\epsilon+\omega)\}, \tag{C3}$$

which coincides with Eq. (47) in the main text. Taking into account (19) and (44), it is clear that there are many contributions to the kernel. For example, if we limit ourselves to the linear approximation, then using the first term in (19), we readily obtain

$$\mathcal{Q}(\omega,\omega') = -2\pi\delta(\omega-\omega')\left[\frac{i\sigma_D}{8}\int_{-\infty}^{\infty} dE\,\mathrm{Tr}\left\{\hat{\tilde{\mathcal{G}}}^R_E\hat{\mathcal{G}}^K_{E+\omega} + \hat{\mathcal{G}}^K_E\hat{\tilde{\mathcal{G}}}^A_{E+\omega}\right\}\right], \tag{C4}$$

which matches the corresponding expression in [62].

As stated in the main text, we will focus on computing the third harmonic contribution to the current. This means that in expression (C3) we need to single out the contributions which contain terms linear in $\check{g}_1(\epsilon,\epsilon')$:

$$\mathcal{Q}_3(\omega,\omega') = \frac{\sigma_D}{8i}\int_{-\infty}^{\infty} dE\,\mathrm{Tr}\big\{\hat{\tilde{\mathcal{G}}}^R_E\hat{g}^K_1(E+\omega',E+\omega) + \hat{g}^R_1(E,E+\omega-\omega')\hat{\tilde{\mathcal{G}}}^K_{E+\omega}$$
$$+ \hat{g}^K_1(E,E+\omega-\omega')\hat{\tilde{\mathcal{G}}}^A_{E+\omega} + \hat{\tilde{\mathcal{G}}}^K_E\hat{g}^A_1(E+\omega',E+\omega)\big\}. \tag{C5}$$

At this point it proves convenient to change the integration variable from E to $\epsilon = E + \omega'$ in the first and fourth terms under the integral, so that all functions $\hat{g}_1$ have the same arguments:

$$\mathcal{Q}_3(\omega,\omega') = \frac{\sigma_D}{8i}\int_{-\infty}^{\infty} dE\,\mathrm{Tr}\big\{\hat{\tilde{\mathcal{G}}}^R_{E-\omega'}\hat{g}^K_1(E,E+\omega-\omega') + \hat{g}^R_1(E,E+\omega-\omega')\hat{\tilde{\mathcal{G}}}^K_{E+\omega}$$
$$+ \hat{g}^K_1(E,E+\omega-\omega')\hat{\tilde{\mathcal{G}}}^A_{E+\omega} + \hat{\tilde{\mathcal{G}}}^K_{E-\omega'}\hat{g}^A_1(E,E+\omega)\big\}. \tag{C6}$$

Using the ansatz (33), we can immediately separate the contribution which contains the function $\hat{g}^K_{1,\mathrm{an}}$, and then that term defines $\mathcal{Q}_3^{(\mathrm{an})}(\omega,\omega')$, Eq. (49), in the main text. In the second step we also separate the terms which contain the products of retarded and advanced Green's functions, which define $\mathcal{Q}_3^{(\mathrm{reg1})}(\omega,\omega')$, Eq. (50). Finally, the remaining term contains the products of the advanced and retarded Green's functions, $\mathcal{Q}_3^{(\mathrm{reg2})}(\omega,\omega')$.

APPENDIX D: THIRD HARMONIC CONTRIBUTION TO THE CURRENT

In this Appendix we provide the expressions for the third harmonic contribution of the response kernel $\mathcal{Q}_3(2\Omega,\omega_\mathrm{p})$.

1. Anomalous contribution

We start with the anomalous contribution $\mathcal{Q}_3^{(\mathrm{an})}$, which is given by the sum of the following two functions:

$$\begin{aligned}\mathcal{Q}_{3,Q}^{(\mathrm{an})}(\Omega,\omega_\mathrm{p}) &= \frac{\pi\sigma_D}{4i}\int_{-\infty}^{\infty}\frac{i\delta W_Q dE}{\zeta_E^R+\zeta_{E+2\Omega}^A}\mathrm{Tr}\big\{\big[\big(\hat{\mathcal{G}}^R_{E+\Omega}-\hat{\mathcal{G}}^R_E\hat{\mathcal{G}}^R_{E+\Omega}\hat{\mathcal{G}}^A_{E+2\Omega}\big)(n_{E+\Omega}-n_{E+2\Omega})\\ &\quad+\big(\hat{\mathcal{G}}^A_{E+\Omega}-\hat{\mathcal{G}}^R_E\hat{\mathcal{G}}^A_{E+\Omega}\hat{\mathcal{G}}^A_{E+2\Omega}\big)(n_E-n_{E+\Omega})\big]\big(\hat{\mathcal{G}}^R_{E-\omega_\mathrm{p}}+\hat{\mathcal{G}}^A_{E+2\Omega+\omega_\mathrm{p}}\big)\big\},\\ \mathcal{Q}_{3,\Delta}^{(\mathrm{an})}(\Omega,\omega_\mathrm{p}) &= \frac{\pi\sigma_D}{4i}\Delta_1(2\Omega)\int_{-\infty}^{\infty}\frac{(n_E-n_{E+2\Omega})}{\zeta_E^R+\zeta_{E+2\Omega}^A}\\ &\quad\times\mathrm{Tr}\big\{\big(\hat{\Xi}_2-\hat{\mathcal{G}}^R_E\hat{\Xi}_2\hat{\mathcal{G}}^A_{E+2\Omega}\big)\big(\hat{\mathcal{G}}^R_{E-\omega_\mathrm{p}}+\hat{\mathcal{G}}^A_{E+2\Omega+\omega_\mathrm{p}}\big)\big\}dE.\end{aligned}\tag{D1}$$

Note that the second contribution has a prefactor $\Delta_1(2\Omega)/\delta W_Q\gg 1$ (Fig. 2), and therefore, we may expect that $\mathcal{Q}_{3,\Delta}^{(\mathrm{an})}$ will significantly exceed $\mathcal{Q}_{3,Q}^{(\mathrm{an})}$ in a range of frequencies when $\Omega\sim\Delta$. The traces of the matrices entering into these expressions can be computed in a straightforward manner. To make the expressions below as compact as possible, we will use the notations $E'=E-\omega_\mathrm{p}$ and $E''=E+2\Omega+\omega_\mathrm{p}$. Recall that $\hat{\Xi}_2\hat{\Xi}_2=-\hat{\mathbb{1}}$ and $\hat{\Xi}_3\hat{\Xi}_2=\hat{\Xi}_1$. It then follows that

$$\begin{aligned}\mathcal{Q}_{3,\Delta}^{(\mathrm{an})}(\Omega,\omega_\mathrm{p}) = i\pi\sigma_D\Delta_1(2\Omega)\int_{-\infty}^{\infty}\frac{(n_{E+2\Omega}-n_E)}{\zeta_E^R+\zeta_{E+2\Omega}^A}&\big\{\big(g_E^R f_{E+2\Omega}^A+f_E^R g_{E+2\Omega}^A\big)\big(g_{E'}^R+g_{E''}^A\big)\\ &+\big(g_E^R g_{E+2\Omega}^A+f_E^R f_{E+2\Omega}^A+1\big)\big(f_{E'}^R+f_{E''}^A\big)\big\}dE.\end{aligned}\tag{D2}$$

A similar, although much lengthier, expression is found for $\mathcal{Q}_{3,Q}^{(\mathrm{an})}$:

$$\begin{aligned}\mathcal{Q}_{3,Q}^{(\mathrm{an})}(\Omega,\omega_\mathrm{p}) &= -\pi\sigma_D\delta W_Q\int_{-\infty}^{\infty}\frac{(n_{E+\Omega}-n_{E+2\Omega})}{\zeta_E^R+\zeta_{E+2\Omega}^A}\big\{G^{RA}_{E'E''}\big[f^R_{E+\Omega}\big(g_E^R f_{E+2\Omega}^A+f_E^R g_{E+2\Omega}^A\big)\\ &\quad+g^R_{E+\Omega}\big(g_E^R g_{E+2\Omega}^A+f_E^R f_{E+2\Omega}^A-1\big)\big]+F^{RA}_{E'E''}\big[f^R_{E+\Omega}\big(g_E^R g_{E+2\Omega}^A+f_E^R f_{E+2\Omega}^A+1\big)\\ &\quad+g^R_{E+\Omega}\big(g_E^R f_{E+2\Omega}^A+f_E^R g_{E+2\Omega}^A\big)\big]\big\}dE-\pi\sigma_D\delta W_Q\int_{-\infty}^{\infty}\frac{(n_E-n_{E+\Omega})}{\zeta_E^R+\zeta_{E+2\Omega}^A}\big\{G^{RA}_{E'E''}\big[f^A_{E+\Omega}\\ &\quad\times\big(g_E^R f_{E+2\Omega}^A+f_E^R g_{E+2\Omega}^A\big)+g^A_{E+\Omega}\big(g_E^R g_{E+2\Omega}^A+f_E^R f_{E+2\Omega}^A-1\big)\big]+F^{RA}_{E'E''}\big[f^A_{E+\Omega}\\ &\quad\times\big(g_E^R g_{E+2\Omega}^A+f_E^R f_{E+2\Omega}^A+1\big)+g^A_{E+\Omega}\big(g_E^R f_{E+2\Omega}^A+f_E^R g_{E+2\Omega}^A\big)\big]\big\}dE.\end{aligned}\tag{D3}$$

Here we use the shorthand notations $G^{RA}_{E'E''}=g^R_{E'}+g^A_{E''}$ and $F^{RA}_{E'E''}=f^R_{E'}+f^A_{E''}$. At temperatures close to absolute zero in order to simplify the numerical calculations we can approximate $n_{E+\Omega}-n_{E+2\Omega}\approx 2[\vartheta(-E-2\Omega)-\vartheta(-E-\Omega)]$ [here $\vartheta(x)$ is the step function], which for positive values of Ω is nonzero only when $E\in[-2\Omega,-\Omega]$. Analogously, the second integral in (D3) is nonzero for $E\in[-\Omega,0]$. We use these expressions to compute the dependence of $\mathcal{Q}_3^{(\mathrm{an})}(\Omega,\omega_\mathrm{p})$ on ω_p for fixed Ω. In Fig. 8 we show the dependence on the probe frequency of the two terms which contribute to $\mathcal{Q}_3^{(\mathrm{an})}=\mathcal{Q}_{3,\Delta}^{(\mathrm{an})}+\mathcal{Q}_{3,Q}^{(\mathrm{an})}$. Given the definition (37), the first term $\mathcal{Q}_{3,\Delta}^{(\mathrm{an})}$ is determined by $\hat{\rho}_\Delta$ and therefore is proportional to $\Delta_1(2\Omega)$, while the remaining term $\mathcal{Q}_{3,Q}^{(\mathrm{an})}$ must then be proportional to δW_Q. Note that $\mathcal{Q}_{3,\Delta}^{(\mathrm{an})}$ and $\mathcal{Q}_{3,Q}^{(\mathrm{an})}$ enter with opposite signs.

2. Regular contribution

The regular contribution to the kernel is given by expressions (50). We start by considering the following expression:

$$\mathcal{Q}_3^{(\mathrm{reg1},R)}(\omega,\omega')=\frac{\sigma_D}{8i}\int_{-\infty}^{\infty}\mathrm{Tr}\big\{\hat{g}_1^R(E,E+\omega-\omega')\big[\hat{\mathcal{G}}^R_{E-\omega'}n_{E+\omega-\omega'}+\hat{\mathcal{G}}^R_{E+\omega}n_{E+\omega}\big]\big\}dE.\tag{D4}$$

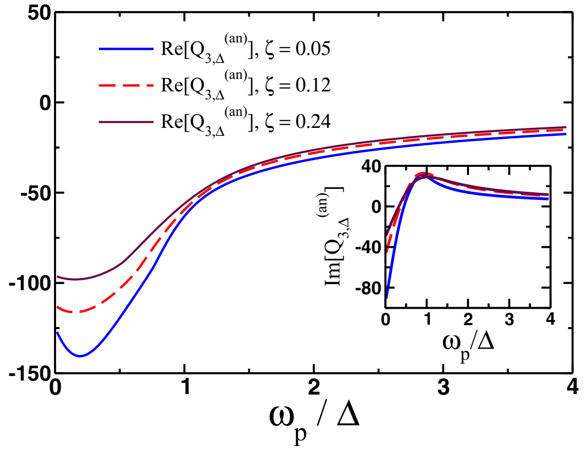

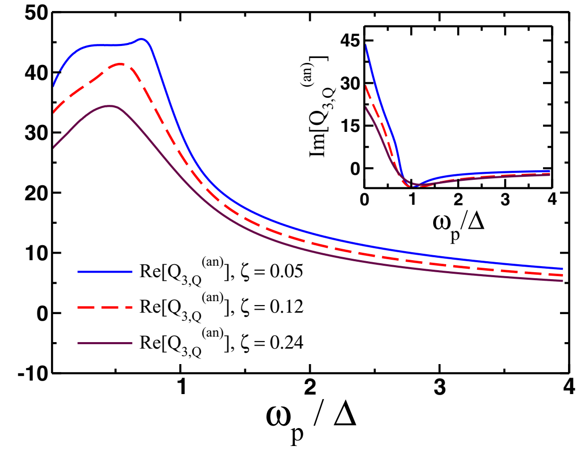

FIG. 8. Plots of the real (main plot) and imaginary (inset) parts of the functions $\mathcal{Q}_{3,\Delta}^{(\mathrm{an})}(\Omega,\omega_\mathrm{p})$ (left panel) and $\mathcal{Q}_{3,Q}^{(\mathrm{an})}(\Omega,\omega_\mathrm{p})$ (right panel) as a function of the probe frequency with the value of the pump frequency fixed to $\Omega = 0.895\Delta$ for various values of the dimensionless parameter ζ. Both functions are given in units of $\delta W_Q \sigma_D$. Note that function $\mathcal{Q}_{3,Q}^{(\mathrm{an})}$ reaches its maximum values at $\omega_\mathrm{p} \approx \Delta_\mathrm{th}$.

Using the definitions (26) from the main text, after some tedious algebraic manipulations similar to the ones used in the derivation of (D3) we find

$$\begin{aligned}\mathrm{Tr}\{\hat{g}_1^R(E,E+2\Omega)\hat{\mathcal{G}}_{E-\omega_\mathrm{p}}^R\} = &-\frac{8\pi i\delta W_Q}{\zeta_E^R+\zeta_{E+2\Omega}^R}\{g_{E+\Omega}^R g_{E-\omega_\mathrm{p}}^R(g_E^R g_{E+2\Omega}^R + f_E^R f_{E+2\Omega}^R - 1) + f_{E+\Omega}^R f_{E-\omega_\mathrm{p}}^R(g_E^R g_{E+2\Omega}^R + f_E^R f_{E+2\Omega}^R + 1)\\ &+ (g_E^R f_{E+2\Omega}^R + f_E^R g_{E+2\Omega}^R)(g_{E+\Omega}^R f_{E-\omega_\mathrm{p}}^R + f_{E+\Omega}^R g_{E-\omega_\mathrm{p}}^R)\}\\ &+\frac{8\pi i\Delta_1(2\Omega)}{\zeta_E^R+\zeta_{E+2\Omega}^R}\{f_{E-\omega_\mathrm{p}}^R(g_E^R g_{E+2\Omega}^R + f_E^R f_{E+2\Omega}^R + 1) + g_{E-\omega_\mathrm{p}}^R(g_E^R f_{E+2\Omega}^R + f_E^R g_{E+2\Omega}^R)\}.\end{aligned} \tag{D5}$$

A similar expression can be easily obtained for the second term in (D4) by replacing $g_{E-\omega_\mathrm{p}}^R$ with $g_{E+2\Omega+\omega_\mathrm{p}}^R$ and $f_{E-\omega_\mathrm{p}}^R$ with $f_{E+2\Omega+\omega_\mathrm{p}}^R$. Since expression (D4) contains the functions which are analytic in the upper half plane of the complex variable E, we replace the integral over E with the summation over the fermionic Matsubara frequencies just like above. We repeat the same procedure for the term which contains only the advanced functions. Finally, essentially the same type of trace as in (D5) needs to be computed in order to evaluate $\mathcal{Q}_3^{(\mathrm{reg2},R)}(\omega,\omega')$. We will not list the resulting expression here. The dependence of these functions on ω_p is presented in Fig. 3 in the main text.

[1] J. A. Fülöp, L. Pálfalvi, G. Almási, and J. Hebling, Design of high-energy terahertz sources based on optical rectification, Opt. Express **18**, 12311 (2010).
[2] D. N. Basov, R. D. Averitt, D. van der Marel, M. Dressel, and K. Haule, Electrodynamics of correlated electron materials, Rev. Mod. Phys. **83**, 471 (2011).
[3] R. Matsunaga and R. Shimano, Nonequilibrium BCS state dynamics induced by intense terahertz pulses in a superconducting NbN film, Phys. Rev. Lett. **109**, 187002 (2012).
[4] R. Matsunaga, Y. I. Hamada, K. Makise, Y. Uzawa, H. Terai, Z. Wang, and R. Shimano, Higgs amplitude mode in the BCS superconductors $Nb_{1-x}Ti_xN$ induced by terahertz pulse excitation, Phys. Rev. Lett. **111**, 057002 (2013).
[5] R. Matsunaga, N. Tsuji, H. Fujita, A. Sugioka, K. Makise, Y. Uzawa, H. Terai, Z. Wang, H. Aoki, and R. Shimano, Light-induced collective pseudospin precession resonating with Higgs mode in a superconductor, Science **345**, 1145 (2014).
[6] M. Beck, I. Rousseau, M. Klammer, P. Leiderer, M. Mittendorff, S. Winnerl, M. Helm, G. N. Gol'tsman, and J. Demsar, Transient increase of the energy gap of superconducting NbN thin films excited by resonant narrow-band terahertz pulses, Phys. Rev. Lett. **110**, 267003 (2013).
[7] G. Eliashberg, Film superconductivity stimulated by a high-frequency field, Sov. Phys. JETP Lett. **11**, 114 (1970).
[8] T. M. Klapwijk, J. N. van den Bergh, and J. E. Mooij, Radiation-stimulated superconductivity, J. Low Temp. Phys. **26**, 385 (1977).
[9] B. I. Ivlev, S. G. Lisitsyn, and G. M. Eliashberg, Nonequilibrium excitations in superconductors in high-frequency fields, J. Low Temp. Phys. **10**, 449 (1973).
[10] A. F. Volkov and S. M. Kogan, Collisionless relaxation of the energy gap in superconductors, Zh. Eksp. Teor. Fiz. **65**, 2038 (1974) [Sov. Phys. JETP **38**, 1018 (1974)].
[11] V. P. Galaiko, Kinetic equation for relaxation processes in superconductors, Sov. Phys. JETP **34**, 203 (1972).
[12] Y. M. Galperin, V. I. Kozub, and B. Z. Spivak, Dissipationless BCS dynamics with large branch imbalance, Sov. Phys. JETP **54**, 1126 (1981).

[13] J. Demsar, B. Podobnik, V. V. Kabanov, T. Wolf, and D. Mihailovic, Superconducting gap Δ_c, the pseudogap Δ_p, and pair fluctuations above T_c in overdoped $Y_{1-x}Ca_xBa_2Cu_3O_{7-\delta}$ from femtosecond time-domain spectroscopy, Phys. Rev. Lett. **82**, 4918 (1999).
[14] R. A. Kaindl, M. Woerner, T. Elsaesser, D. C. Smith, J. F. Ryan, G. A. Farnan, M. P. McCurry, and D. G. Walmsley, Ultrafast mid-infrared response of $YBa_2Cu_3O_{7-\delta}$, Science **287**, 470 (2000).
[15] R. D. Averitt, G. Rodriguez, A. I. Lobad, J. L. W. Siders, S. A. Trugman, and A. J. Taylor, Nonequilibrium superconductivity and quasiparticle dynamics in $YBa_2Cu_3O_{7-\delta}$, Phys. Rev. B **63**, 140502(R) (2001).
[16] G. L. Warner and A. J. Leggett, Quench dynamics of a superfluid Fermi gas, Phys. Rev. B **71**, 134514 (2005).
[17] A. Pashkin, M. Porer, M. Beyer, K. W. Kim, A. Dubroka, C. Bernhard, X. Yao, Y. Dagan, R. Hackl, A. Erb, J. Demsar, R. Huber, and A. Leitenstorfer, Femtosecond response of quasiparticles and phonons in superconducting $YBa_2Cu_3O_{7-\delta}$ studied by wideband terahertz spectroscopy, Phys. Rev. Lett. **105**, 067001 (2010).
[18] M. Beck, M. Klammer, S. Lang, P. Leiderer, V. V. Kabanov, G. N. Gol'tsman, and J. Demsar, Energy-gap dynamics of superconducting NbN thin films studied by time-resolved terahertz spectroscopy, Phys. Rev. Lett. **107**, 177007 (2011).
[19] U. Eckern, A. Schmid, M. Schmutz, and G. Schön, Stability of superconducting states out of thermal equilibrium, J. Low Temp. Phys. **36**, 643 (1979).
[20] P. B. Littlewood and C. M. Varma, Amplitude collective modes in superconductors and their coupling to charge-density waves, Phys. Rev. B **26**, 4883 (1982).
[21] R. T. Brierley, P. B. Littlewood, and P. R. Eastham, Amplitude-mode dynamics of polariton condensates, Phys. Rev. Lett. **107**, 040401 (2011).
[22] D. Pekker and C. Varma, Amplitude/Higgs modes in condensed matter physics, Annu. Rev. Condens. Matter Phys. **6**, 269 (2015).
[23] A. Moor, A. F. Volkov, and K. B. Efetov, Amplitude Higgs mode and admittance in superconductors with a moving condensate, Phys. Rev. Lett. **118**, 047001 (2017).
[24] R. Shimano and N. Tsuji, Higgs mode in superconductors, Annu. Rev. Condens. Matter Phys. **11**, 103 (2020).
[25] R. A. Barankov, L. S. Levitov, and B. Z. Spivak, Solitons and Rabi oscillations in a time-dependent BCS pairing problem, Phys. Rev. Lett. **93**, 160401 (2004).
[26] M. H. Szymanska, B. D. Simons, and K. Burnett, Dynamics of the BCS-BEC crossover in a degenerate Fermi gas, Phys. Rev. Lett. **94**, 170402 (2005).
[27] E. A. Yuzbashyan, B. L. Altshuler, V. B. Kuznetsov, and V. Z. Enolskii, Solution for the dynamics of the BCS and central spin problems, J. Phys. A **38**, 7831 (2005).
[28] E. A. Yuzbashyan, B. L. Altshuler, V. B. Kuznetsov, and V. Z. Enolskii, Nonequilibrium cooper pairing in the nonadiabatic regime, Phys. Rev. B **72**, 220503 (2005).
[29] E. A. Yuzbashyan, V. B. Kuznetsov, and B. L. Altshuler, Integrable dynamics of coupled Fermi-Bose condensates, Phys. Rev. B **72**, 144524 (2005).
[30] R. A. Barankov and L. S. Levitov, Dynamical selection in developing fermionic pairing, Phys. Rev. A **73**, 033614 (2006).
[31] L. D. Landau, On the vibrations in the electronic plasma, J. Phys. (Moscow) **10**, 25 (1946).
[32] B. B. Kadomtsev, Landau damping and echo in a plasma, Sov. Phys. Usp. **11**, 328 (1968).
[33] V. Gurarie, Nonequilibrium dynamics of weakly and strongly paired superconductors, Phys. Rev. Lett. **103**, 075301 (2009).
[34] E. A. Yuzbashyan, M. Dzero, V. Gurarie, and M. S. Foster, Quantum quench phase diagrams of an *s*-wave BCS-BEC condensate, Phys. Rev. A **91**, 033628 (2015).
[35] E. A. Yuzbashyan, O. Tsyplyatyev, and B. L. Altshuler, Relaxation and persistent oscillations of the order parameter in fermionic condensates, Phys. Rev. Lett. **96**, 097005 (2006); Erratum: Relaxation and persistent oscillations of the order parameter in fermionic condensates [Phys. Rev. Lett. **96**, 097005 (2006)] **96**, 179905(E) (2006).
[36] E. A. Yuzbashyan, Normal and anomalous solitons in the theory of dynamical Cooper pairing, Phys. Rev. B **78**, 184507 (2008).
[37] P. Derendorf, A. F. Volkov, and I. M. Eremin, Nonlinear response of diffusive superconductors to ac electromagnetic fields, Phys. Rev. B **109**, 024510 (2024).
[38] For details on this issue we refer the reader to the discussion in Sec. V of Ref. [34].
[39] T. Papenkort, V. M. Axt, and T. Kuhn, Coherent dynamics and pump-probe spectra of BCS superconductors, Phys. Rev. B **76**, 224522 (2007).
[40] T. Papenkort, T. Kuhn, and V. M. Axt, Nonequilibrium dynamics and coherent control of BCS superconductors driven by ultrashort THz pulses, J. Phys.: Conf. Ser. **193**, 012050 (2009).
[41] H. Krull, D. Manske, G. S. Uhrig, and A. P. Schnyder, Signatures of nonadiabatic BCS state dynamics in pump-probe conductivity, Phys. Rev. B **90**, 014515 (2014).
[42] N. Tsuji and H. Aoki, Theory of Anderson pseudospin resonance with Higgs mode in superconductors, Phys. Rev. B **92**, 064508 (2015).
[43] A. F. Kemper, M. A. Sentef, B. Moritz, J. K. Freericks, and T. P. Devereaux, Direct observation of Higgs mode oscillations in the pump-probe photoemission spectra of electron-phonon mediated superconductors, Phys. Rev. B **92**, 224517 (2015).
[44] T. Cea, C. Castellani, and L. Benfatto, Nonlinear optical effects and third-harmonic generation in superconductors: Cooper pairs versus Higgs mode contribution, Phys. Rev. B **93**, 180507(R) (2016).
[45] Y.-Z. Chou, Y. Liao, and M. S. Foster, Twisting Anderson pseudospins with light: Quench dynamics in terahertz-pumped BCS superconductors, Phys. Rev. B **95**, 104507 (2017).
[46] P. W. Anderson, Knight shift in superconductors, Phys. Rev. Lett. **3**, 325 (1959).
[47] M. Silaev, Nonlinear electromagnetic response and Higgs-mode excitation in BCS superconductors with impurities, Phys. Rev. B **99**, 224511 (2019).
[48] G. Seibold, M. Udina, C. Castellani, and L. Benfatto, Third harmonic generation from collective modes in disordered superconductors, Phys. Rev. B **103**, 014512 (2021).
[49] R. Haenel, P. Froese, D. Manske, and L. Schwarz, Time-resolved optical conductivity and Higgs oscillations in two-band dirty superconductors, Phys. Rev. B **104**, 134504 (2021).
[50] F. Yang and M. W. Wu, Impurity scattering in superconductors revisited: Diagrammatic formulation of the supercurrent-supercurrent correlation and Higgs-mode damping, Phys. Rev. B **106**, 144509 (2022).

[51] F. Yang and M. W. Wu, Influence of scattering on the optical response of superconductors, Phys. Rev. B **102**, 144508 (2020).

[52] A. I. Larkin and Y. N. Ovchinnikov, Density of states in inhomogeneous superconductors, Sov. Phys.- JETP **34**, 1144 (1972).

[53] M. Dzero and A. Levchenko, Spatially inhomogeneous magnetic superconductors, Phys. Rev. B **104**, L020508 (2021).

[54] D. Sherman, U. S. Pracht, B. Gorshunov, S. Poran, J. Jesudasan, M. Chand, P. Raychaudhuri, M. Swanson, N. Trivedi, A. Auerbach, M. Scheffler, A. Frydman, and M. Dressel, The Higgs mode in disordered superconductors close to a quantum phase transition, Nat. Phys. **11**, 188 (2015).

[55] A. Kapitulnik, S. A. Kivelson, and B. Spivak, Colloquium: Anomalous metals: Failed superconductors, Rev. Mod. Phys. **91**, 011002 (2019).

[56] M. Dzero, M. Khodas, and A. Levchenko, Transport anomalies in multiband superconductors near the quantum critical point, Phys. Rev. B **108**, 184513 (2023).

[57] M. Dzero, Collisionless dynamics in disordered superconductors, arXiv:2303.06750.

[58] A. A. Abrikosov and L. P. Gor'kov, Contribution to the theory of superconducting alloys with paramagnetic impurities, Sov. Phys. JETP **12**, 1243 (1961).

[59] A. V. Balatsky, I. Vekhter, and J.-X. Zhu, Impurity-induced states in conventional and unconventional superconductors, Rev. Mod. Phys. **78**, 373 (2006).

[60] A. Lamacraft and B. D. Simons, Tail states in a superconductor with magnetic impurities, Phys. Rev. Lett. **85**, 4783 (2000).

[61] A. Lamacraft and B. D. Simons, Superconductors with magnetic impurities: Instantons and subgap states, Phys. Rev. B **64**, 014514 (2001).

[62] Y. V. Fominov, M. Houzet, and L. I. Glazman, Surface impedance of superconductors with weak magnetic impurities, Phys. Rev. B **84**, 224517 (2011).

[63] M. A. Skvortsov and M. V. Feigel'man, Subgap states in disordered superconductors, J. Exp. Theor. Phys. **117**, 487 (2013).

[64] Y. Yerin, A. A. Varlamov, and C. Petrillo, Topological nature of the transition between the gap and the gapless superconducting states, Europhys. Lett. **138**, 16005 (2022).

[65] V. M. Galitski and A. I. Larkin, Spin glass versus superconductivity, Phys. Rev. B **66**, 064526 (2002).

[66] R. A. Barankov and L. S. Levitov, Excitation of the dissipationless Higgs mode in a fermionic condensate, arXiv:0704.1292.

[67] M. Dzero, E. A. Yuzbashyan, and B. L. Altshuler, Cooper pair turbulence in fermionic atom traps, Europhys. Lett. **85**, 20004 (2009).

[68] H. Gao, F. Schlawin, and D. Jaksch, Higgs mode stabilization by photoinduced long-range interactions in a superconductor, Phys. Rev. B **104**, L140503 (2021).

[69] M. V. Feigel'man, A. I. Larkin, and M. A. Skvortsov, Keldysh action for disordered superconductors, Phys. Rev. B **61**, 12361 (2000).

[70] A. Kamenev and A. Levchenko, Keldysh technique and nonlinear σ-model: Basic principles and applications, Adv. Phys. **58**, 197 (2009).

[71] A. Kamenev, *Field Theory of Non-equilibrium Systems* (Cambridge University Press, Cambridge, UK, 2011).

[72] Y. Lu, S. Ilić, R. Ojajärvi, T. T. Heikkilä, and F. S. Bergeret, Reducing the frequency of the Higgs mode in a helical superconductor coupled to an LC-circuit, Phys. Rev. B **108**, 224517 (2023).

[73] F. M. Marchetti and B. D. Simons, Tail states in disordered superconductors with magnetic impurities: The unitarity limit, J. Phys. A **35**, 4201 (2002).

[74] M. Kharitonov, T. Proslier, A. Glatz, and M. J. Pellin, Surface impedance of superconductors with magnetic impurities, Phys. Rev. B **86**, 024514 (2012).

Correction: Support information in the second sentence in the Acknowledgment section has been fixed.